

**A NEW APPROACH TO MODELLING FLOODING IMPACTS ON
EMERGENCY SERVICE ACCESSIBILITY: A CASE STUDY OF
CALGARY, ALBERTA**

**A NEW APPROACH TO MODELLING FLOODING IMPACTS ON
EMERGENCY SERVICE ACCESSIBILITY: A CASE STUDY OF
CALGARY, ALBERTA**

By

MICHELE TSANG, B.Sc.

A Thesis

Submitted to the School of Graduate Studies

In Partial Fulfillment of the Requirements

For the Degree

Master of Science

McMaster University

© Copyright by Michele Tsang, September 2019

MASTER OF SCIENCE (2019)

McMaster University

(School of Geography and Earth Sciences)

Hamilton, Ontario, Canada

TITLE: A new approach to modelling flooding impacts on emergency
service accessibility: A case study of Calgary, Alberta

AUTHOR: Michele Tsang, B.Sc. (McMaster University)

SUPERVIOR: Dr. Darren M. Scott

NUMBER OF PAGES: x, 87

Abstract

Floods are becoming more frequent and the magnitude of direct consequences, relating to destruction of critical infrastructure and loss of life, has highlighted the importance of flood management. This thesis proposes a new methodology to quantify the impact of predicted and historic flooding events on emergency services. The approach moves beyond simple flood inundation mapping by accounting for the relationship between flood depth and vehicular speed. A case study was presented for Calgary Alberta, where the depths of a predicted 100-year flood and an historic 2013 flood event were modelled. The methodology applied geographic information systems (GIS) to flood depth mapping, utilizing digital elevation models (DEMs), flood extents, and hydrological data. Flood depths were then assigned to links comprising the road network, where the maximum vehicle speed was calculated as a function of the standing depth of water on a link. The flooded network was used to derive service areas for several types of emergency services (emergency medical services (EMS), fire, and police), following targeted response times. The results quantified and located the residential and work populations that no longer meet the targeted response times. During both flood scenarios, EMS were found to have the greatest reduction in accessibility, with 23% to 47% of residents and workers, respectively, not served. Fire services were seen to be more resilient with only 3% to 9% of residents and workers, respectively, not served. The results for police services were similar to fire services. However, the former have a greater range of response times, meaning these areas represent those that are completely isolated during both flood events. Overall, the proposed methodology quantified vulnerable populations on a partially degraded network, which can

be used to develop evacuation plans and emergency response strategies, minimizing disturbances in the network and the number of people affected.

Acknowledgements

First and foremost, I would like to thank my supervisor Dr. Darren Scott for giving me the opportunity to pursue my Master's degree. This thesis project would not be possible without his support and guidance. His expertise in the field of GIS and transportation science has allowed me to grow in my academic career.

I would also like to thank my TransLAB mates, Matt Brown, Jayden Choi, Nosheen Alamgir, and Christina Boroweic, for their help and advice during graduate school. They have always made the research lab a comfortable environment to work and discuss issues.

Finally, I would like to thank my friends and family for their support throughout this journey. I am incredibly grateful for the endless love and support from my parents and brother. Last but not least, I would like to thank Ryan for his love, encouragement, and guidance in both the academic and personal aspects of my life.

Table of Contents

Abstract	iii
Acknowledgements	v
List of Tables	viii
List of Figures	ix
Glossary	x
1. Chapter 1: Introduction	1
2. Chapter 2: Background	9
2.1. Vulnerability	9
2.2. Accessibility	11
2.3. Emergency Response	13
2.4. Flood Network Modelling	15
2.5. Flood Mapping Using GIS	17
3. Chapter 3: Objectives	21
4. Chapter 4: Study Area and Data	23
4.1. Study Area	23
4.1. Flood Mapping	25
4.1.1. Predicted Flood	26
4.1.2. Historic Flood	26
4.2. Population	27
4.3. Land Use	29
4.4. Emergency Response Services	30
5. Chapter 5: Methods	31
5.1. Flood Depth Mapping	31
5.1.1. Predicted Flood	31
5.1.2. Historic Flood	33
5.2. Flooded Network	36
5.3. Service Areas	40

5.4. Population.....	42
6. Results and Discussion	44
6.1. Population Statistics	44
6.1.1. EMS	44
6.1.2. Fire	50
6.1.3. Police.....	54
6.2. Network Statistics	57
6.3. Research Contributions	60
6.3.1. Accessibility Modelling	60
6.3.2. Flood Inundation Mapping	62
7. Chapter 7: Summary and Conclusion	65
7.1. Summary of Findings	65
7.2. Limitations	67
7.3. Concluding Remarks	69
8. References.....	71
9. Appendix.....	86

List of Tables

Table 1. Number of residents and workers served before a flood event.....	44
Table 2. Residential, dependent and work populations not served.....	46
Table 3. Number and length (km) of links affected during the 100-year and 2013 flood.	58
Table 4. Number and length (km) of each type of link affected.....	59
Table 5. Overestimation of non-accessible individuals following the base case conditions.....	62

List of Figures

Figure 1. Study area and road network of Calgary, Alberta.	28
Figure 2. Deriving the depth of a (A) predicted and (B) historic flood.	33
Figure 3. Flood extents and links affected from a (A) 100-year flood and the (B) 2013 flood.	37
Figure 4. Base case representing (A) residents and (B) workers served by EMS within the 12-minute threshold.	45
Figure 5. (A) Residents and (B) workers not served by EMS following the 12-minute threshold during a 100-year flood.	48
Figure 6. (A) Residents and (B) workers not served by EMS following the 12-minute threshold during the 2013 flood.	49
Figure 7. (A) Residents and (B) workers not served by fire following the 12-minute threshold during the 100-year flood.	52
Figure 8. (A) Residents and (B) workers not served by fire following the 12-minute threshold during the 2013 flood.	53
Figure 9. (A) Residents and (B) workers not served by police following the 120-minute threshold during the 100-year flood.	55
Figure 10. (A) Residents and (B) workers not served by police following the 120-minute threshold during the 2013 flood.	56
Figure 11. Validation of 2013 flood extent by comparing overlap of reference data.	63
Figure 12. Base case representing (A) residents and (B) workers served by fire within the 12-minute threshold.	86
Figure 13. Base case representing (A) residents and (B) workers served by police within the 120-minute threshold.	87

Glossary

Erase	Creates a feature class by overlaying the input features with the polygons of the erase features. Only those portions of the input features falling outside the erase features outside boundaries are copied to the output feature class.
Euclidean Allocation	Calculates, for each cell, the nearest source based on Euclidean distance.
Extract By Mask	Extracts the cells of a raster that correspond to the areas defined by a mask.
Intersect	Computes a geometric intersection of the input features. Features or portions of features which overlap in all layers and/or feature classes will be written to the output feature class.
Polygon To Raster	Converts polygon features to a raster dataset.
Raster Calculator	Builds and executes a single Map Algebra expression using Python syntax in a calculator-like interface.

Chapter 1: Introduction

In Canada, floods are the most common natural hazard and also among the costliest (Public Safety Canada, 2019a). The increased frequency of flooding events in recent decades has been linked to rapid urban expansion and changes in precipitation patterns caused by anthropogenic climate change (Hirabayashi et al., 2013; Katz et al., 2002; Vogel et al., 2011; Yang et al., 2015; Kundzewicz et al., 2019; Kunkel et al., 1999; Nirupama and Simonovic, 2006; Peterson et al., 2008). Climate change scenario projections for Canada estimate an increase in temperatures between $4.9^{\circ}\text{C} \pm 1.7^{\circ}\text{C}$ and $6.6^{\circ}\text{C} \pm 2.3^{\circ}\text{C}$ by 2050, depending on different emission scenarios (IPCC, 2013; Poesch et al., 2016). This warming, which is progressing more rapidly in Canada than in other parts of the world, is accompanied by increases in precipitation (Westra et al., 2014), streamflow (Novotny and Stefan, 2007), snowmelt (Pederson et al., 2011), and extreme flooding events (Vincent et al., 2015). Floods most commonly occur when rivers or streams overflow their banks due to excessive runoff following rainfall events. Historically, development in close proximity to water was crucial for survival, due to the access of drinking water, water transportation, and fertile land for agriculture (Elshorbagy et al., 2016). In other regions, residing near water has more aesthetic, cultural or recreational value (Kummu et al., 2011). In Canada, human occupancy on floodplains is a historical phenomenon that will likely persist in the future because of the extensive urbanization that already exists and the poor understanding of flood risk maps (de Loe, 2008; McClearn, 2019). Urbanization increases the rate of runoff as the removal of vegetation and soil decreases areas of water storage. The significant reduction of infiltration leads to higher flood peaks and volumes, even for low

duration rainfall events (Westra et al., 2014). The United Nations (UN) states that 55% of the world's population is currently living in urban areas, which is expected to increase to 68% by 2050 (United Nations, 2018). North America is no exception as it is one of the highest urbanized regions in the world, with 82% of its population living in urban areas (United Nations, 2018). Critical infrastructure, which refers to transportation networks, protection services (such as police or military), community services, government services, and utility networks, is crucial to the functioning of cities (Sharma et al., 2008). Disruption from flooding to such infrastructure puts the health, safety, security, and economic well-being of individuals at risk, as observed in New Orleans, following hurricane Katrina (Pistrika and Jonkman, 2009); and southern Alberta, due to heavy rainfall and snowmelt during the spring of 2013. The migration of people from rural to urban areas amid the growing frequency of natural disasters magnifies difficulties in assessing risk and managing appropriate emergency response (Smith et al., 2014; Price and Vojinovic, 2008). In order for cities to become more resilient to flooding, consequences relating to risk of life (Lane et al., 2013; Jonkman et al., 2009), property damage (Lee and Kim, 2017; Brody et al., 2007; Sande et al., 2003), and failure of infrastructure (Singh et al., 2018; Sohn, 2006; Jongman et al., 2012) must be minimized (Hammond et al., 2013).

In Canada, transportation infrastructure is essential to the country's economic growth and social interactions (Public Safety Canada, 2019b). Reliable transportation infrastructure is vital to the functioning of modern societies as people and businesses plan their everyday lives with the assumption to travel and transport goods between different places (Mattson, 2007). In Canada, the road network is the dominant type of transportation

infrastructure for facilitating the movement of people, goods, and services (Transport Canada, 2018). Such networks have continued to expand, becoming increasingly complex in response to urban development and growing populations. In urban areas, these networks provide access to work, education, business, and recreation, while acting as vital lifelines connecting isolated communities in rural areas (Taylor and D’Este, 2003). As society’s reliance on the network and expectation of its performance grows, so do the consequences of network failure (Taylor and D’Este, 2003). Historical events have shown that road networks are vulnerable to natural disasters, such as earthquakes (Chang and Nojima, 2001; Cho et al., 2001), floods (Coles et al., 2017, Novak and Sullivan, 2014; Yin et al., 2016; Suarez et al., 2005), forest fires (Dimopoulou and Giannikos, 2004), and hurricanes (Horner and Widener, 2011; Chen et al., 2006). Network failures and disruptions threaten opportunities for people to receive medical care and other critical services (Jenelius and Mattsson, 2015). These unpredictable events also cause other severe consequences relating to the road network, such as increased traffic congestion, cancellation of trips, and inaccessible destinations (Suarez et al., 2005). It is important to study these consequences as they affect people’s daily lives and the economy. Methods and decision support tools allow planners and policy makers to make rational assessments during threats to facilities and infrastructure (Taylor and D’Este, 2003).

The detrimental effects of flooding and their increase in occurrence has highlighted the need for more effective flood management. Previous studies have sought to assess potential flooding impacts. Such studies have focused on emergency evacuation (Alsnih and Stopher, 2004; Church and Cova, 2000), risk of inundated links (Yin et al., 2016),

network resilience (Yucel et al., 2018), accessibility loss (Sohn, 2016), flash floods (Balijepalli and Oppong, 2014), satisfying demand (Jenelius et al., 2006), socio economic impacts (Taylor and Susilawati, 2012), and measuring the relative importance of links with respect to their system-wide contribution to traffic flow (Novak and Sullivan, 2014). Koenig (1980) identified accessibility as a key concept in urban and transport planning, referring to the ease of opportunities for interaction or exchange. It provides a sound tool for evaluating the effectiveness of transport plans and policies, especially at a disaggregate level, when considering cost and benefits derived by users, environmental effects, accidents, or indirect effects on land use (Koenig, 1980). The structure and capacity of the urban transportation network directly affects the level of accessibility, which is crucial to urban planning and emergency response (Zhu and Liu, 2004). When a disaster occurs, not all links will respond the same way as some will have a greater impact on network flows relative to others. It is also important to acknowledge that when a link is disrupted, it does not necessarily mean that it completely fails. The ability to plan for and manage the impacts of network degradation allows for cities to remain connected during unpredictable events.

Public Safety Canada helps Canadians and their communities protect themselves from emergencies and natural disasters through the development and implementation of policies, plans, and a range of programs (Public Safety Canada, 2019c). The approach to emergency management is based on four related areas: prevention and mitigation, emergency preparedness, responding to emergency events, and recovery from disasters. Prevention and mitigation are the efforts to reduce impacts of disasters and associated financial costs. Emergency preparedness refers to the efforts taken prior to an emergency,

which include planning and testing of emergency management arrangements. Responding to emergency events provides assistance before, during, or after disasters by first responders, such as medical professionals and hospitals, fire departments, police, and municipalities, which warn and evacuate communities. Recovery from disasters are the efforts to recover from emergencies and their consequences. This thesis aims to address two of these areas: prevention and mitigation, and emergency preparedness. Mapping flood extents allows for affected populations to be located and quantified. People can then take precautions to minimize damage to their properties and evacuate to areas where they are no longer at risk. In regards to emergency preparedness, flood maps reflecting events of a specified magnitude provide insight on those most vulnerable for officials. Identifying potentially affected populations can be used to allocate services and resources in more efficient ways. Additionally, taking action in these two areas indirectly optimizes responding to emergency events as there may be fewer people who may need assistance during a disaster. This can also make the recovery process more effortless as the risk of individuals and damage to properties may be reduced or prevented. Implementing strategies before a disaster occurs is the best way to minimize both direct impacts, relating to personal injury or property damage, and indirect impacts, such as disruption to public services or economic activities, of flooding events (Yin et al., 2016).

The goal of emergency services is to protect and save lives by responding safely and quickly. Longer response times may result in more losses, indicating inadequate service (Indriasari et al., 2010). Quicker response times may save more lives and properties from casualties and damages. Denser urban networks improves accessibility but for emergency

services, specific targets must be met. Therefore, emergency facility location and response problems are typically modeled under time or distance constraints (Coles et al. 2017; Novak and Sullivan, 2014; Shiomi et al., 2011; Yang et al., 2006). The threat of natural disasters, such as flooding, is also enhanced due to the concentration of people in large cities, placing more people at risk when resources are limited. Several studies have attempted to identify vulnerable populations during flooding events by integrating geographic information systems (GIS) with accessibility modelling (e.g., Coles et al., 2017; Green et al., 2017; Indriasari et al., 2010). Using a network analysis, GIS allows for service areas to be derived while taking into account road access, barriers, and network attributes, providing solutions to prevent and respond to these flooding disasters. A network service area is a region that encompasses all accessible streets, within the specified impedance. Many studies have used GIS to determine service areas for multiple purposes, including recreation (Oh and Jeong, 2007), health care (McLafferty, 2003; Yang et al., 2006), and transit planning (Mavoa et al., 2012). Identifying service areas is a simple and straightforward approach to implement, which can be executed around any location on a network. Regarding emergency planning, these locations are typically emergency facilities, such as EMS stations, fire stations, police stations, hospitals, or health clinics. This study uses the capabilities of GIS to improve upon the current service area methods by considering barriers of different magnitudes depending on flood depth. The spatial capabilities provided by GIS serves as a powerful tool for decision makers, who are responsible for the safety of lives, properties, and environments during flooding disasters.

Despite recent efforts to evaluate the effectiveness of road networks during flooding, assumptions in the development and application impact the accuracy when assessing the consequences. This research evaluates the accessibility of emergency services during flooding events, which can be modelled using the partial or complete degradation of links. The methodology augments previous studies where links in the network were either considered flooded to a threshold where travel was prohibited anywhere along the link or the link was not affected by flooding at all (Coles et al., 2017; Green et al., 2017; Yin et al., 2016). This study uses an equation derived by Pregolato et al. (2017) to analyze partially operating roads along with those completely failing, as a function of water depth. To apply this in the context of accessibility modelling, GIS is used to generate service areas of emergency services. The maximum speed of emergency vehicles is calculated with respect to the depth of water on a network link, illustrating more realistic conditions and providing better estimates of areas that can and cannot be reached within targeted response times. This paper focuses on urban cities prone to flooding. These areas are vulnerable to climate change as they are likely to experience both the influence of river discharge and surface runoff. Due to the close proximity of rivers and water bodies, Calgary, Alberta was selected as the case study.

The remainder of this thesis is organized as follows: The following chapter reviews literature regarding relevant concepts: trip simulation, flood mapping methods, and the importance of emergency response strategies. Chapter 3 describes the main objectives of the research by integrating flood mapping, network analysis, emergency response, and accessibility modelling. Chapter 4 provides some historical context of the study area,

Calgary, and why it is relevant to flooding. In Chapter 5, the methodology in deriving flood inundation maps is presented. The steps in determining flood extents and depths are explained, followed by how this data is used to create flooded road networks. Chapter 6 presents the results based on two flooding events: a predicted 100-year flood and a recreation of the historic 2013 Alberta flood. The thesis concludes with Chapter 7, explaining how this research contributes to existing studies regarding accessibility modelling and inundation mapping, as well as the limitations and assumptions.

Chapter 2: Background

Transportation research is extensive and encompasses many disciplines, but the aim of providing better transportation systems and services has continued to be an important area (Sun and Yin, 2017). This study focuses on emergency planning and response, as the reoccurring floods in Canada have highlighted the need for research in this field. This chapter defines important terms used, vulnerability and accessibility, as these concepts are not only valuable in modelling network changes but also serves great importance in measuring social impacts. To address these consequences of flooding, current maps, equations, and models were evaluated in order to determine the best techniques that can be feasibly applied in this study. By focusing on these areas, the performance of networks were analyzed based on the failure of components, as well as the wider social impacts on those served by the network

2.1. Vulnerability

Vulnerability is a commonly used term to assess the impacts and damages of flooding on the road network (Jenelius and Mattsson, 2015; Balica et al., 2012; Taylor et al., 2006; Chen et al., 2015; Lu et al., 2015; Balijepalli and Oppong, 2014). This concept has been heavily discussed in the literature, but the definition varies between authors. Many suggest that there is no single definition suitable for vulnerability, but it is defined based on the context of the event. One of the most accepted definitions was introduced by Berdica (2002), who suggested vulnerability in the road transportation system is the susceptibility to incidents that can result in considerable reductions in road network serviceability. These

events can be unpredictable and range in severity caused by weather, physical failures, traffic accidents, planned road works, or terrorist actions (Berdica, 2002). Other studies have associated vulnerability with the concept of risk (Hall et al., 2003; Nicholson and Dalziell, 2003). The term “risk” contains two components: the probability of an event occurring and the consequences arising due to the event (Kasperson et al., 1988). This definition was followed by Jenelius et al. (2006), who identified critical road links in terms of link importance and local exposure, based on the increase in generalized cost of travel for journeys in degraded networks. Chen et al. (2015) also agreed with this as network vulnerability was quantified based on the probability of sea level rise. Erath et al. (2009) considered both the probability of the natural hazard and the indirect consequences, such as the changes in travel time and distance, to determine route choice effects during link failures. Other authors defined flood risk using physical based modelling, considering flow analysis, hydraulic modelling, and precipitation (Balica et al., 2012; Afshari et al., 2018; Karmakar et al., 2010) However, it has been acknowledged that including the probability of failure in vulnerability introduces difficulty when trying to estimate the probability of rare events, such as natural disasters (Sarewitz et al., 2003).

From a different perspective, road network vulnerability analysis can be defined as the study of potential degradations on the network and their impacts on society (Jenelius and Mattsson, 2015). Taylor and Susilawati (2012) defined network vulnerability relating to the consequences of failure of some component on the network, such as a link or node, irrespective to the probability of failure. Even if the probability of a component failure is low, the social and economic impacts may be sufficiently large, suggesting that the low

probability of occurrence may not offset the consequence of network failure (D'Este and Taylor, 2001). Sarewitz et al. (2003) also argued that the concept of vulnerability should be independent from probability as probabilities of extreme events are difficult to estimate and are constantly changing. Understanding and reducing vulnerability does not demand accurate prediction of extreme events as it can be evaluated by focusing on the social disruptions during the aftermath of disasters. The authors agree that the concept of vulnerability should be viewed separately from risk as this thesis analyzed vulnerability with concerns to the consequences instead of probabilities. Here, consequences refer to the partial and complete failure of links and populations without access to emergency services.

2.2. Accessibility

An early and well-known definition of accessibility was defined by Hansen (1959) as the potential of opportunities for interaction. Similarly, Niemeier (1997) defined accessibility as the ease with which desired destinations may be reached. These broad definitions can be narrowed to be context-specific and include relevant factors, such as time constraints and travel modes. Geurs and Wee (2004) explain accessibility extensively, consisting of four components: land use, transportation, time, and individual. Paez et al. (2012) defined accessibility as being comprised of two components: the cost of travel and the quality/quantity of opportunities. Many authors view vulnerability as reduced accessibility (Taylor et al., 2006; Chen et al., 2015; Sohn, 2016). Our definition of accessibility is most similar to that by Coles et al. (2017) who quantified accessibility based on the coverage of emergency responders. In this paper, we measured accessibility based

on the populations that were served by emergency services dispatched from known locations.

The accessibility of road networks has been a growing research field over the past few decades, for transportation planning, urban planning, and emergency management. O’Sullivan et al. (2000) defined the goal of any transport system as the access to facilities, where they evaluated the transport system as the effectiveness of delivering people to desired facilities. Many studies that measured accessibility used well-developed indices, such as the Hansen Accessibility index, or some form of it (Chen et al., 2015; Lu and Peng, 2011; Taylor et al., 2006). Lu and Peng (2011) improved on the Hansen Accessibility Index by accounting for the population of each travel zone with respect to the entire population of the study area. Sohn (2016) derived an accessibility index to incorporate the distance-decay effect and the volume of traffic influence on the transportation network. Novak and Sullivan (2014) created a measure for evaluating the accessibility provided by each link with respect to the link’s system-wide relationship to all emergency service facilities in a roadway network. Lu et al. (2015) used an accessibility-based methodology to evaluate the network-wide impacts of infrastructure degradation based on the increase in travel cost, destination attractiveness, and traffic congestion. Chang (2010) defined an accessibility performance measure to determine the time it takes to restore rail accessibility back to normal following a disaster. Bono and Gutierrez (2011) looked at reduced accessibility following earthquakes by removing disrupted road segments and disconnecting roads where there were point disruptions. While these methods are useful for accessibility analyses, the outcome focused on the effects of the network and did not provide impacts on

the population. Miller (1999) states that transportation planning should focus specifically on the changes in accessibility, as it determines the winners and losers in a given scenario. This was demonstrated by Coles et al. (2017), who developed a method that coupled flood modelling with network analysis to evaluate the accessibility of emergency responders to care homes and sheltered accommodation. Similar to Coles et al. (2017), this study evaluates the accessibility of emergency services during flooding events using GIS. However, we consider the entire population of the city instead of focusing on elders living in support homes. This study also improves on the previous methodology by allowing for travel on partially flooded links.

2.3. Emergency Response

Evaluating network degradation in combination with emergency services is a growing field of interest as the connectivity of road links is vital for emergency vehicles to have access to residences and other populated areas (Chen et al., 2015; Coles et al., 2017; Novak and Sullivan, 2014; Albano et al., 2014). Shiomi et al. (2011) used an accessibility-based index to evaluate the vulnerability of road networks to natural disasters to determine optimal allocation of medical facilities. Viswanath and Peeta (2003) sought routes for emergency services that minimized travel time and maximized the population covered. Unpredictable natural disasters and the geographic variation in population provides the need for analysis and planning of emergency access. McLafferty (2007) defined need as a multidimensional concept that is based on peoples' characteristics, behaviors, and environments in which they live and work. Populations are not spread evenly across the

Earth's surface, affecting their access to opportunities. People also differ in age, gender, and economic status, which affects their need for specific services (McLafferty, 2007). Sene (2008) emphasized that emergency response during floods should have special arrangements made for the dependent population (elderly and children) and those disabled. These populations may not be able to physically ensure their own safety, making them more vulnerable. Coles et al. (2017) also recognized this and analyzed the vulnerability of care homes and sheltered accommodation, based on targeted response times of emergency services. Their results stated the response time to each care home and sheltered accommodation and the number of locations not meeting the thresholds. However, the capacity and number of occupants could differ drastically, resulting with a greater number of elders impacted for some locations. Albano et al. (2014) estimated total populations at risk and the proportion of children and elderly during flooding events. Similarly, this thesis seeks to address not only the total number of people affected by flooding, but also quantifies the number of dependents affected, defined by those ages 19 and under and 65 and above. The method differs from Albano et al. (2014) as they distributed populations homogeneously within census areas.

Smith et al. (2019) compared 30 meter (m), 90 m, and 900 m flood exposure maps, where a decrease in resolution resulted in a greater overestimation of populations within flood inundation zones. This thesis provides high resolution population distributions as the residential population is assigned to residential lands within census areas (DAs), while work populations are assigned to commercial lands within census area. Accounting for the work population, which the authors have yet to identify in the literature, provides valuable

insights on where workers are during the day. Therefore, results from this study quantifies the number of people affected from flooding, during any time of the day.

2.4. Flood Network Modelling

People's safety can be compromised when vehicles traveling on inundated roads lose traction or become buoyant (Shah et al., 2019). When modelling floods, a critical threshold is typically used by researchers to determine if the road is flooded to a depth where cars can no longer safely travel. Shah et al. (2019) developed safety guidelines for vehicle stability on flooded surfaces based on experimental and analytical data, where small passenger, large passenger, and large 4WD vehicles cannot navigate in depths greater than 0.3 m, 0.4 m, and 0.5 m, respectively. Other authors modelled the effects of flooding on the network with reduced capacity (Chen et al., 2015; Balijepalli and Oppong, 2014). Balijepalli and Oppong (2014) used historical data to identify links prone to flooding during two scenarios. The first scenario reflected a minor flood, where flood prone links were reduced by a capacity of 20%, while the second scenario represented a moderate size flood, where flood prone links were reduced by a capacity of 50%. Similarly, Chen et al. (2015) simulated four flooding scenarios caused by sea level rise, where capacity was reduced for all flooded links in the network. Scenario one represented the base case, where the network was not degraded. Scenario two, three, and four reduced the flooded link capacities by 50%, 99%, and 100%, respectively. However, both studies assumed that all flooded links were affected the same way in these scenarios. Therefore, the guidelines provided by Shah et al.

(2019) can be utilized to model floods in a more realistic way as travel on flooded links is based on the depth of water.

Based on the characteristics of different types of vehicles and forces acting upon the vehicle during a flood, many authors have applied a threshold of 30 centimeters (cm) to restrict travel on flooded links (Kramer et al., 2016; Martinez-Gomariz et al., 2017; Pregolato et al., 2017; Yin et al., 2016). However, when roads are inundated at depths less than 30 cm, they are assumed to operate normally (Coles et al., 2017; Green et al., 2017; Yin et al., 2016; Chen et al., 2015). The effects of flooding on road links is viewed as binary, where 30 cm defines flooded links, preventing travel, while anything less than that does not affect links at all. This assumption may underestimate travel times as depths less than 30 cm may force vehicles to drive at reduced speeds. Another assumption used by researchers prevents travel on all links within predicted flood extents, rendering them useless (Suarez et al., 2005). However, this does not necessarily mean the link is inundated to a magnitude where it is not operational, as travel may be allowed at a lower speed.

When links in the network become flooded, they are not all affected the same and should not be treated that way. Floods will have a greater impact on specific links in the network, based on location and elevation. Pregolato et al. (2017) developed a depth-disruption function, derived by reviewing and combining data from experimental, observational, and modelling studies, that models the relationship between the depth of standing water and vehicle speed. This equation allows for a more realistic treatment of inundated links as they can be analyzed partially, instead of restricting travel completely. Singh et al. (2018) used the equation by Pregolato et al. (2017) to identify critical links by

calculating the reduction in speed across the network during a flood. Similar to this thesis, 10-year and 100-year flood maps were initially overlaid on the road network to determine flooded links. Vulnerable road segments were classified based on the magnitude of reduction in average maximum speed, while resilient roads were defined as those that did not change in speed. This thesis also uses the depth-disruption function developed by Pregolato et al. (2017) as the maximum speed for any link in the network can be calculated based on the standing depth of water. This is applied in the context of emergency services as emergency response routes are simulated based on the shortest travel time from a station to a destination. This improves on previous methods where routes with the shortest distance are assumed to have the shortest response times, as emergency vehicles are not required to obey speed limits (Albano et al., 2014). Even though this is true, the depth of water on a link still has the potential to reduce the speed of emergency vehicles as they are not immune to the drag and buoyancy forces caused by water flow. Network failures, either full or partial, should mirror reality as much as possible or else negative impacts may not be captured.

2.5. Flood Mapping Using GIS

The development of raster-based flood models combined with high resolution digital elevation models (DEMs) and multispectral images makes it possible to accurately model historical and predicted flooding events. Multiple approaches for flood mapping exist in the literature, differing upon data inputs, such as elevation, land use, probability, rainfall, and geomorphic characteristics, such as channel geometry and flow (Albano et al., 2014;

Elshorbagy et al., 2017; Brivio et al., 2010; Youssef and Pradhan, 2011). In the context of emergency planning, GIS software can provide improvements to warning, evacuation, and response by optimizing emergency vehicle routes and locating emergency response facilities (Karmakar et al., 2010; Chakraborty et al., 2005; Coles et al., 2017; Green et al., 2017; Indriasari et al., 2010). McCarthy et al. (2007) found that models of inundation extent were useful to emergency responders when planning for evacuations or deciding where to allocate resources. Brivio et al. (2010) applied a simple approach using GIS techniques to estimate flood extents with a DEM and satellite image. Flood extents were determined using a least accumulative cost-distance matrix where river cells were assumed to flow out of the river channel to reach flooded areas shown on the satellite image. Like the methods used in this thesis, Brivio et al.'s. (2010) approach required the same data inputs, but did not output information about the depth of the flood at each cell.

Rennó et al. (2008) developed a quantitative topographic algorithm called height above nearest drainage (HAND) from a DEM. The topography data provided by a DEM can define where water will accumulate in an area based on flow direction and speed. All grid points belonging to the drainage network were zeroed in height and used as a topographic reference. Elshorbagy et al. (2017) developed a terrain descriptor similar to HAND called elevation above nearest drainage (EAND), executed through ArcGIS. Pixel values in a DEM represent altitudes relative to local drainage instead of the mean sea level. Flood hazard maps were developed for all of Canada using two parameters: EAND and the distance from nearest drainage, the horizontal distance from the nearest drainage network. Schnebele et al. (2014) simulated a historic flood using a 30 m DEM and a 3.2 m satellite

image collected on the day of a flood. Supervised classification was then used on the satellite image to identify water pixels. Corresponding pixels in the DEM with a height less than the mean river height during the flood were set to flood pixels to approximate the extent. Similar to Rennó et al. (2008), Schnebele et al. (2014) and Elshorbagy et al. (2017), flooded cells in this study were derived based on their relative elevation with respect to the drainage network. The terrain descriptor, EAND, is adopted in this study but differs from Elshorbagy et al. (2017) as the drainage network is not calculated from flow direction (Rennó et al., 2008). Instead, the drainage network is defined by major waterbodies only and does not consider intermittent streams. The analysis resolves issues related to resolution, such as averaging values and missing data, as a one meter DEM is applied. Additionally, these errors can propagate through DEM-derived products, including slope, aspect, or flow accumulation, and subsequently affect the interpretation of these results (Holmes et al., 2000). The use of a high resolution DEM provides a more precise representation of the surface, while maintaining topographic attributes of the landscape.

Afshari et al. (2018) evaluated the use of recently developed low-complexity methods, which required only one or two data inputs, to model flooding conditions. These methods, such as HAND and AutoRoute, were compared with a more complex hydrodynamic model (Hydrologic Engineering Center-River Analysis System 2D), which required stream flow, flow equations, surface roughness, and channel and flood plain cross-sections. Inundation extents resulting from all three models were compared for 10-year, 100-year and 500-year flooding scenarios. The low-complexity flood models did not perform as well but gave comparable results and overall, could be considered as a suitable

alternative for fast predictions. Despite the accuracy of hydrodynamic models, Jafazadegan and Merwade (2019) also recognized the computational demand required and believed topography data provided by DEMs allowed for optimal solutions in floodplain mapping at much lower costs. The size of the study area, desired accuracy of the flood maps, computational and monetary costs of modelling, and the type of modelling are some factors that control the methods executed and defined as appropriate (Jafazadegan and Merwade, 2019).

This research contributes to the literature by introducing a simple method to derive flood inundation maps, providing information about the depth and extent of a flood. Any flooding event can be derived using a DEM and flood parameter, which is the flood extent or height of the flood. To the authors' knowledge, the methodology presented in this paper to derive flood depths has yet to be introduced in the literature. This straightforward approach allows for flood mapping to be integrated into network and accessibility analysis by considering the relationship between water depth and vehicle speed. The results can provide insights into the populations potentially impacted by flooding, defined by those not accessible by emergency services, helping decision makers to take necessary precautions to minimize the number of people affected.

Chapter 3: Objectives

This research has two objectives: (1) to propose and demonstrate a new methodology for measuring the accessibility of emergency services during a flooding event that accounts for a partially degraded network, and (2) to quantify the populations affected by said event. This study integrates flood extent mapping, flood depth modelling, network analysis, accessibility of emergency services, and the vulnerability of populations, which has yet to be completed in the literature. While these perspectives are not new, it is the integration that provides a new approach for accessibility modelling during flooding events. This study utilizes the relationship between water depth and vehicle speed when measuring the accessibility of emergency services, which some have failed to recognize (Coles et al., 2017; Green et al., 2017; Yin et al., 2016). Investigating how modelling accessibility of emergency services can be improved provides valuable insight into the effectiveness of emergency planning and the performance of transportation infrastructure.

Flood depth mapping serves as a useful tool for spatial planning of the development of a city, as infrastructure and drainage systems are key to keeping the population resilient to flooding events. However, the data and computational requirements are often too demanding for predictions, as the extensive requirement of inputs are often not readily available. The method proposed in this study requires a DEM and a single flood parameter, the predicted flood extent or the maximum height of water during the flood. This is similar to existing techniques in the literature, but requires fewer parameters and data processing steps (Elshorbagy et al., 2017; Rennó et al., 2008; Schnebele et al., 2014). Service areas are then established considering the flooded road network and spatial distribution of residential

and working populations. This study builds on models where population was distributed based on dissemination areas (DA), census tracts, travel analysis zones, or other geographical units (Lu and Peng, 2011; Albano et al., 2014). Here, populations are further proportioned from these subdivisions based on land use, instead of assuming they are distributed uniformly within a geographical unit. Thus, residential and working populations are only assigned to residential and commercial areas, respectively. The development of high resolution population datasets combined with recently created flood inundation maps provides accurate locations and estimates of populations vulnerable to flooding.

The new methodology introduced for flood depth mapping is applied in the context of emergency response. The results provide vital information for emergency service and facility location decisions, evacuation procedures, and emergency route planning to accommodate populations that are at a disadvantage (Coles et al., 2017; Novak and Sullivan, 2014; Indriasari et al., 2010; Albano et al., 2014). There is a significant gap in understanding the interaction of flooded networks and their effects on population. Research regarding the location of populations and the impacts of flooding disasters on them should be prioritized as much as predicting the magnitude and frequency of such events. Not only does this study quantify and locate populations vulnerable to flooding, but it also considers the dependent population who may have limited physical capabilities. Evaluating the performance of emergency services aids in the development of strategic emergency planning to provide better service and builds safer communities for any city.

Chapter 4: Study Area and Data

4.1. Study Area

Historically, the most disastrous floods in Canada, in terms of the estimated total costs in dollars, have occurred where major river systems intersect densely populated areas (Burton, 2015). The city of Calgary (census subdivision) is no exception as it is centered where the Bow and Elbow rivers meet, while being home to 1.2 million people (Statistics Canada, 2016). The Bow River originates from the Rocky Mountains, winding through the mountains, foothills, and prairies of Alberta (Veiga et al., 2015). Even though the city's road network is dense, seen in Figure 1, the impact of natural disasters and extreme weather events are largely determined by population concentration (Jenelius and Mattsson, 2012). In addition, the close proximity of the city to the Rocky Mountains presents a challenge in accurate weather forecasting as forecasters often have trouble predicting how weather systems behave once they reach the mountains (City of Calgary, 2018a).

Fluvial flooding can occur at any time of the year in Calgary; however, the period between May 15 and July 25 is historically when the city receives the largest amount of rainfall (City of Calgary, 2018a). June is typically the wettest month of the year, when the mountain snowmelt begins to appear on the prairies (Environment and Climate Change Canada, 2017). The combination of heavy rains, melting snow packs in the Rocky Mountains, and the steep and rocky terrain causes rapid and intense flooding in the city (City of Calgary, 2018b). In the spring of 2013, Calgary experienced the largest flood it has seen since 1932 (City of Calgary, 2018b). This disastrous event was caused by a combination of the geography of the region and the extreme weather conditions that lasted

over three days (Milrad et al., 2013). Precursor events leading up to the flood began with a thick, mountain snowpack in May, measuring over one meter at some locations (Environment and Climate Change Canada, 2017). This was followed with a large spring snowmelt, saturating the soil and filling rivers and streams (Environment and Climate Change Canada, 2017). The triggering factor was the torrential rainfall from June 19 to June 21, giving Calgary 68 mm of rain over 48 hours (Environment and Climate Change Canada, 2017). Despite flood mitigation strategies employed by the city, such as lowering the water level of the Glenmore Reservoir to maximize the quantity of water captured and temporary flood barriers throughout critical locations in the city, the Bow and Elbow rivers topped their banks (City of Calgary, 2018b).

Evacuation orders began on June 20 for low-lying areas of Calgary, followed by a complete evacuation of downtown Calgary on June 21, as water levels continued to rise (Calgary Herald, 2013). Emergency response was required across 32 communities in Calgary (city) and the downtown area was inaccessible for days (City of Calgary, 2018b). Emergency crews used helicopters, boats, combines, front-end loaders, and manure spreaders to rescue stranded residents (Environment and Climate Change Canada, 2017). Sadly, five lives were lost and 100,000 people were evacuated. Infrastructure loss included 3000 flooded buildings, over a thousand kilometers of destroyed roads, and hundreds of washed away bridges and culverts (Environment and Climate Change Canada, 2017). Financial losses and property damages were estimated to be as much as six billion dollars (City of Calgary, 2018b). The consequences from this devastating event on the city and its

residents emphasizes the importance of flood mitigation as floods cannot be controlled, but preparing for disaster can help a community's resiliency.

The largest floods along the Bow River have occurred due to three factors: a large snowpack, a late spring, and high temperatures with torrential rain (Whitfield and Pomeroy, 2016). These conditions are predicted to become more common in Canada as the mean annual temperature of high-latitude areas has increased by almost twice the rate of the global average (AMAP, 2011; Vincent et al., 2015). Such conditions cause shorter return periods for extreme events, as seen with Calgary, where the city has a 3.9% chance of a 100-year flood occurring in a year, versus 1% (Fletcher, 2018). The magnitude of the 2013 flood was estimated to have a return period around 50 to 100 years (Stanfield, 2019; Thomas, 2013; Sutherland, 2016). Therefore, the 2013 flood was chosen to model the historic flood event due to the evidence of the damages and the increased frequency of occurrence.

4.1. Flood Mapping

The proposed methodology for flood depth mapping is applied to two flooding scenarios in Calgary, a predicted and historic flood event. The predicted flood reflects a 100-year flood, while the historic flood is based on the 2013 Alberta floods. To determine the flood depth of the 100-year flood, a DEM and predicted flood extent is required. For the 2013 flood, the flood depth and extent can be recreated using a DEM, the location of major waterbodies, and the height of water during the peak of the flood.

A one meter DEM of Calgary was obtained from the city of Calgary, collected in 2017. The total extent of the city is comprised of 459 DEMs, which were merged into a single raster. The coordinate system of the raster is NAD 1983 CSRS 3TM 114.

4.1.1. Predicted Flood

One hundred-year flood extents, as well as other probabilities, are publically available on Open Calgary, the city of Calgary's open data portal (Open Calgary, 2018a). The extent of flood shown has a one in one hundred or a 1% chance of occurring in any year. The shapefile was mapped in 2015 by Alberta Environment and Parks and the city of Calgary, using the best available hydrologic and hydraulic data and models (Open Calgary, 2018a). The flooding extent reflects the conditions, hydrology, and topography of 2015 and does not consider mitigation measures, such as changes to reservoirs/dams or barriers built since then (Open Calgary, 2018a). The 100-year flood extent encompasses the floodway, where water is the deepest and has the fastest flow, and the flood fringe, where overland flooding occurs. The flood extent data was initially preprocessed by the authors, removing polygons less than five meters as it is assumed vehicles can navigate through puddles (Coles et al., 2017; Green et al., 2017).

4.1.2. Historic Flood

Historical water height and flow data are publically available from Environment Canada. Daily water levels can be observed by specifying the station location or number and year. On June 21, 2013, the peak water level at the Bow River station gauge was identified as 4.093 meters at its maximum (Government of Canada, 2019). The Bow River

station gauge is located at 51° 03' 00" N, 114° 03' 05" W, which is adjacent to downtown Calgary (Government of Canada, 2019).

Hydrology data, available from Open Calgary, was used to delineate the drainage systems in Calgary. The shapefile includes intermittent and permanent water bodies and water courses (Open Calgary, 2018b). Drainage systems were computed from the flow of water over a given landscape and ultimately represents where water ends up the surface (Curkendall et al., 2003). This research defined drainage systems using only the major waterbodies in Calgary, which are the Bow River, Elbow River, and Glenmore Reservoir.

The 2013 flood extent was also mapped by the city of Calgary, where an aerial photo from June 22, 2013 was used to manually delineate the flood. The flood extent was not used to predict the flood depth, but was instead used to validate the methodology in delineating the historic 2013 flood extent. The aerial photo was taken after the peak of the flood had passed, which may underestimate peak flood extents (City of Calgary, 2018c). Also, errors may have been introduced from the aerial photo, caused by interference of trees and shadows.

4.2. Population

The residential population was obtained from the 2016 census, which is available from Statistics Canada (Statistics Canada, 2019). Each record in the data represents a unique dissemination area (DA) in Calgary. The population for each DA is recorded, as well as the population of various age groups. The age groups include 0-4, 5-9, 10-14, 15-19, 20-24, 25-29, 30-34, 35-39, 40-44, 45-49, 50-54, 55-59, 60-64 and 65+. The work

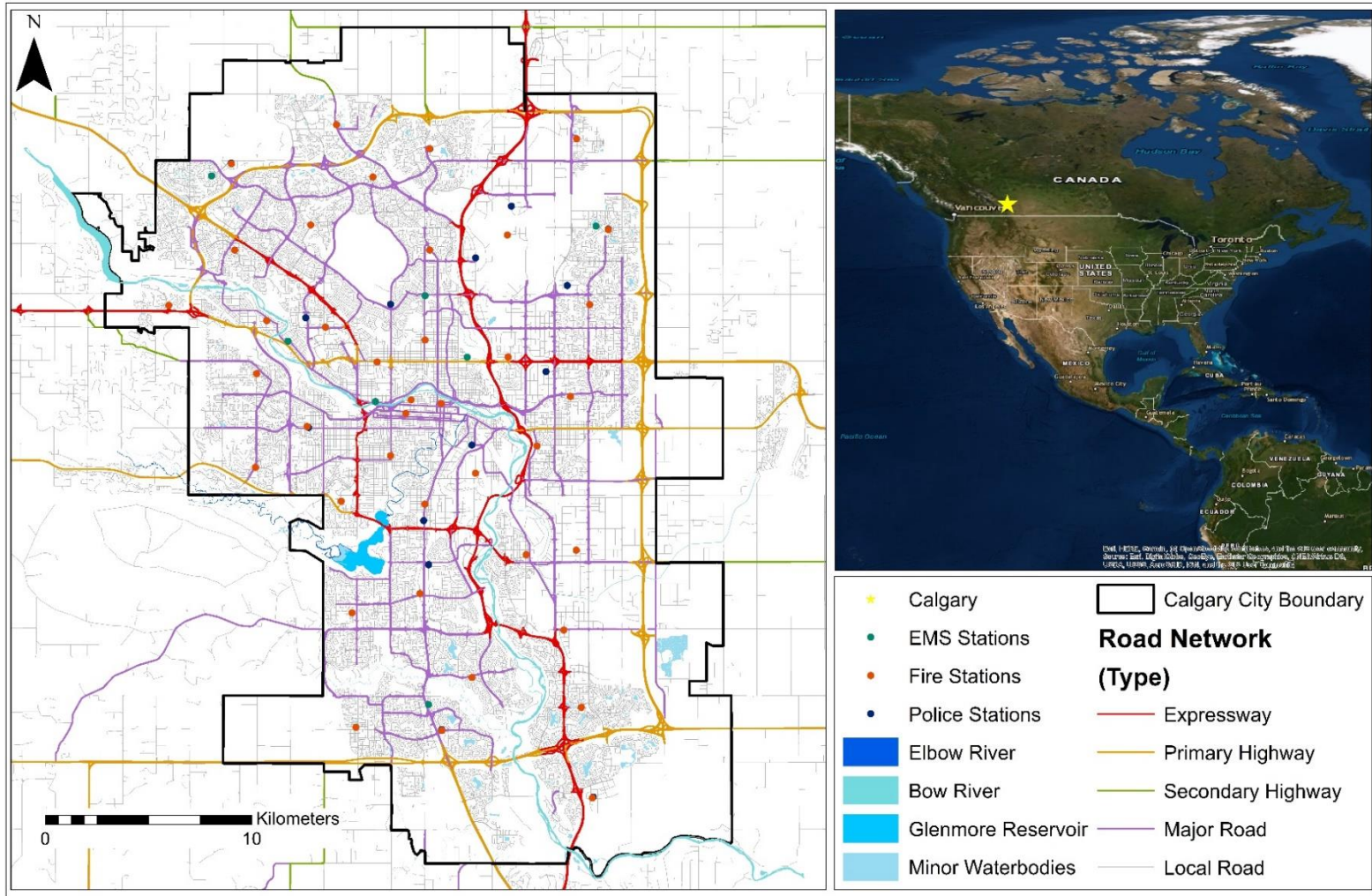


Figure 1. Study area and road network of Calgary, Alberta.

population was obtained from Statistics Canada's Research Data Centre at McMaster University (RDC). The residential population is where individuals live while the work population is where people are working during the day. Looking at the age groups gives additional insights into the types of populations not served within time constraints. Flooding impacts may be magnified for dependent populations, those ages from 0 to 19 and 65 and over, if they have limited, physical capabilities. When identifying vulnerable groups in the United Kingdom, authorities find greater challenges in locating vulnerable individuals in the community, compared to when they are clustered together, such as in care homes or hospitals. (Houston, et al., 2011). The results help predict where areas may be in need of greater assistance, which can be used to promote effective research, policy development, and implementation for dependent populations.

4.3. Land Use

Land use data is also available on Open Calgary. The land use shapefile contains parcel data for land use classes in the City, such as residential, commercial, recreational, and institutional, which is further classified based on density or a more descriptive purpose (Open Calgary, 2018c). This study focuses on residential and work populations so only these corresponding land uses are extracted from the land use dataset.

The Calgary road network, which is shown in Figure 1, was obtained from the CanMap Content Suite, created by DMTI Spatial in 2016.

4.4. Emergency Response Services

The dispatch stations of EMS, fire and police for the city of Calgary can be seen in Figure 1. There are a total of 39 Calgary fire stations, which Calgary firefighters operate 24 hours per day to serve the community, mapped by Open Calgary (2018c). Currently, the targeted response time for fire services is 7 minutes for the city and 12 minutes for rural areas, with proposals to increase the lower bound to 10 minutes (Dippel, 2018). There are a total of 8 EMS stations in Calgary, located by Open Calgary (2018d). In 2015, Alberta Health Services set a new response time target at 12 minutes for urban areas across Alberta, including Calgary, while longer targets were set for rural areas (Yourex, 2015). There are a total of 12 Calgary police service district offices mapped by Open Calgary (2018e). The response time of police depends on the priority level of the call, where the target is 7 minutes for in progress calls with people at risk, 12 minutes for in progress calls for property at risk, 17 minutes for calls that occurred, 40 minutes for time sensitive calls, and lastly 180 minutes for general service (CTV News, 2019). However, since the entire city can be reached within 120 minutes, applying a threshold of 120 and 180 minutes produces the same service areas. Therefore, a threshold of 120 minutes was used as it does not affect the number of people served but provides more specific results.

Chapter 5: Methods

The proposed methodology couples flood mapping with accessibility mapping, using GIS. The availability of high resolution DEMs and land use/cover data allows for accurate flood mapping. The flood maps are integrated with network analysis and applied in the context of emergency response and accessibility modelling. The methods presented are executed through a GIS software package, ArcGIS, and can be applied to any region to evaluate the impacts of flooding. This study demonstrates the methods for Calgary, using parameters characteristic to the city.

5.1. Flood Depth Mapping

Flood depth maps provide more realistic and useful information to flooding on the road network as some links may still be traversed if the water depth is within the recommended depth for safe driving. The new method for flood depth mapping introduces two approaches: how to derive the depth of a predicted flood and how to recreate the extent and depth of a historic flood. The approaches differ by the parameters required and the data processing techniques.

5.1.1. Predicted Flood

The approach in developing a flood depth map for a predicted flood event requires two data inputs: a DEM and a flood extent parameter. The depth of water at any flooded location, d_f , is calculated by computing the difference between the elevation of the flooded

cell, e_f , and the elevation of the closest (based on Euclidean distance) non-flooded cell, e_n , written as:

$$d_f = e_n - e_f \quad (1)$$

The elevation of the flooded cell is determined by identifying the corresponding cell in the DEM. Therefore, the elevation of the closest non-flooded cell must be derived in order to determine the depth of water at the flooded cell, demonstrated in Figure 2A. This example outlines selected flooded cells (light purple and light red) and the closest non-flood cell (purple and red, respectively), where all cells displayed as elevation are not flooded.

Following Equation 1, a flood depth map was created for the city of Calgary, representing a 100-year flood event. Pre-processing of the data was required, such as converting the 100-year flood shapefile to raster format and the DEM into integer format and centimeter units. Next, the extent of the 100-year flood was removed from the DEM using the Raster Calculator, where the cells in the inundation extent were set to NoData. It is also important to note that an assumption made was that any cells outside of the 100-year flood inundation area were not flooded and have a water depth of 0. The Euclidean Allocation tool was then used to identify the closest non-flooded cell, e_n , to each flooded cell, e_f , based on Euclidean distance. When the closest cell was identified, the flooded cell was reassigned the elevation value of the non-flooded cell. In the resulting Euclidean Allocation raster, each flooded cell represents e_n . Lastly, the original DEM, in centimeter units and integer format, was subtracted from the Euclidean Allocation raster, resulting with depths seen in Figure 3A. Negative values can be ignored as they represent peaks in

elevation. All locations outside of the flood extent do not have associate depths. Rivers, symbolized by water in Figure 3, also do not have depth values as roads do not pass through them, allowing them to be ignored in the analysis.

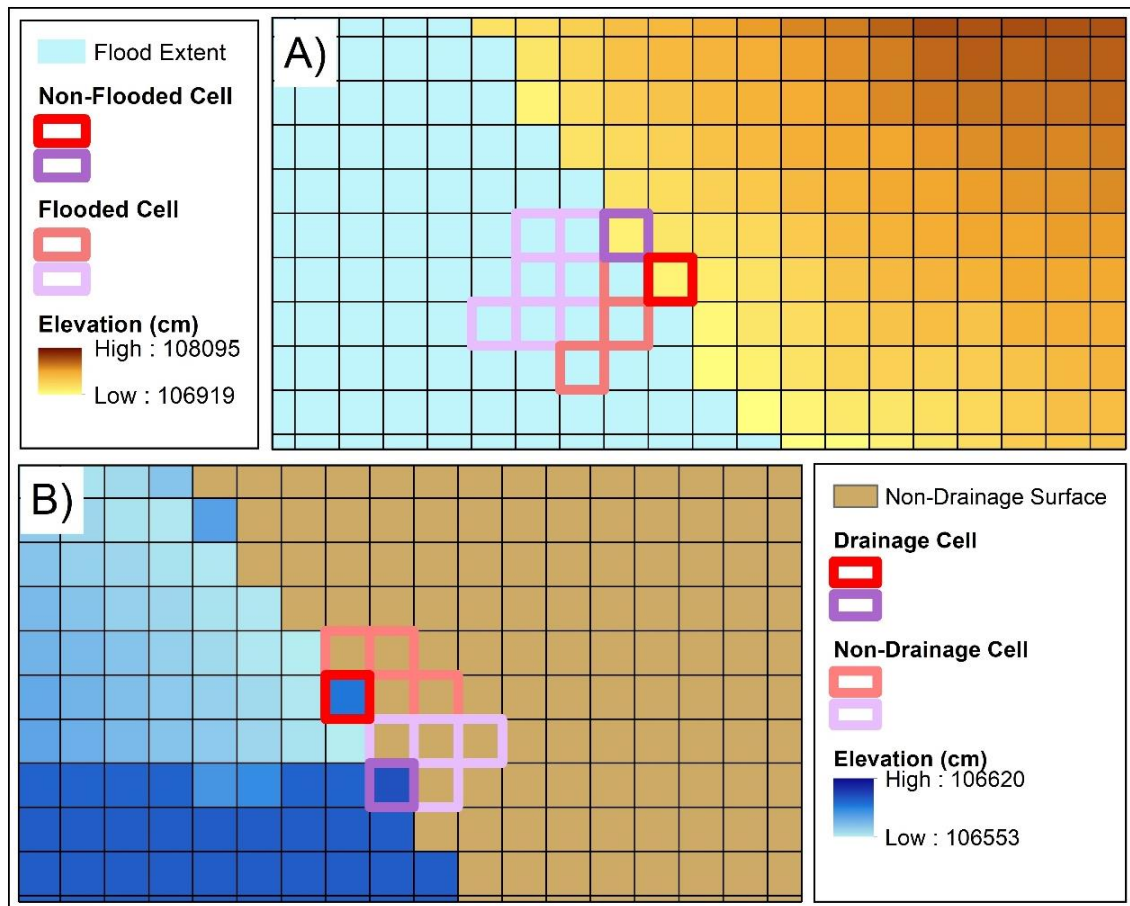


Figure 2. Deriving the depth of a (A) predicted and (B) historic flood.

5.1.2. Historic Flood

The second approach is used to develop a flood depth map for a historic flooding event. Not only does the map predict flood depths, but also the flood extent for any height

of a flood. This approach has two steps: creating an EAND raster and extracting cells of a desired flood height. In the EAND raster, cell values represent elevations relative to the local drainage instead of mean sea level (Elshorbagy et al., 2017). There are three data requirements: a DEM, the extent of drainage systems, and a peak flood height parameter. In this study, the extent of the drainage system represented the river banks. The EAND of any location, $EAND_i$, can be determined by finding the difference between the elevation at such cell, e_i , and the elevation of the closest drainage cell, e_d , written as:

$$EAND_i = e_i - e_d \quad (2)$$

The elevation for location i can be determined by identifying the corresponding cell in the DEM. Therefore, the elevation of the closest drainage cell must be derived to determine the EAND, seen in Figure 2B. Drainage cells were defined by waterbodies while non-drainage cells represented terrain that was initially not flooded. In the second step, cells with an EAND value less than or equal to the height of the peak of the flood were considered flooded. These cells were extracted from the EAND raster to represent the extent of the flood, where each cell value represented the water depth. This study maps fluvial floods, therefore only extracted cells connected to the rivers are considered flooded in the final result.

The 2013 Alberta flood was recreated in the city of Calgary, representing a maximum flood height of four meters. For the first step, the Extract By Mask tool was executed on the DEM and the drainage system, resulting with cells within the drainage extent retaining their value, while the rest became NoData. The Euclidean Allocation tool was used to reassign each NoData cell to the value of the closest drainage cell. In the resulting Euclidean

allocation raster, each cell outside of the drainage extent contained the elevation value of the closest drainage cell, e_d . Lastly, the Euclidean Allocation raster was subtracted from the original DEM, resulting with the EAND raster.

At the Bow River station gauge, adjacent to downtown Calgary, a record high water level was measured at approximately four meters (Government of Canada, 2019). To determine the extent of this flood event, the Select by Attributes tool was used to export cells in the EAND raster equal to or less than 400 cm, seen in Figure 3B. Values greater than 0 represented the depth of water while values equal to 0 represented the drainage system. Negative values represented depressions lower than the drainage systems and were assumed to have a water depth of 400 cm.

A limitation to the flood mapping method is that it is only capable for predicting the depths of a fluvial flood. The historic flood modelled from 2013 was a fluvial flood, which occurs when there is excessive rainfall over an extended period of time, causing rivers to exceed their capacity. Heavy snowmelt from upstream can also promote these fluvial floods. When looking at the resulting four meter flood raster, there are many flooded cells not connected to the river extent. Since this is a fluvial flood, flooded cells should be directly adjacent to the river or connected to ones that are. Flooded cells not connected to the river in any way do not represent the flood extent and are only allocated these values because they are at an elevation lower than the drainage system. Therefore, they must not be viewed as flooded during the 2013 Alberta Flood. To remove the areas not connected to the drainage system, the flooded area must first be converted to a shapefile. The Reclassify tool was then used so that all values would be reclassified to one and NoData remained the

same. An easier step would be to convert the raster directly to a polygon but this was not possible due to the file size of the data, preventing the tool from being executed successfully. Next, the reclassified raster was successfully converted to a polygon as the amount of data was reduced. The Select Layer By Location tool was then executed such that only polygons connected to the river were selected and exported to represent the areas affected by a fluvial flooding event. Now that the flooded extent was accurately identified, the corresponding cells were extracted from the EAND raster.

5.2. Flooded Network

Flood depth maps can be integrated into network analysis by assigning water depths to each location in the road network. Road links were overlaid on the flood depth map, where links intersecting flooded cells were assigned the corresponding depth of water. Since each road link had multiple cells associated with it, the maximum and average depth of water was calculated for each link. The average depth was used to calculate the maximum speed a vehicle can travel along on that link. The maximum depth was used to determine restricted links, therefore, if any point on the road link was greater than or equal to 30 cm of water, the entire link was classified as restricted. The same steps were executed for assigning depths from a predicted and historic flood event.

To assign flood depths to the Calgary road network, the Extract By Mask tool was used to intersect the flood depth raster and with the Calgary road network. The resulting flood depth raster only contained cells that intersected the road network. The flood depth raster was then converted into lines such that it aligned with Calgary's road network. This

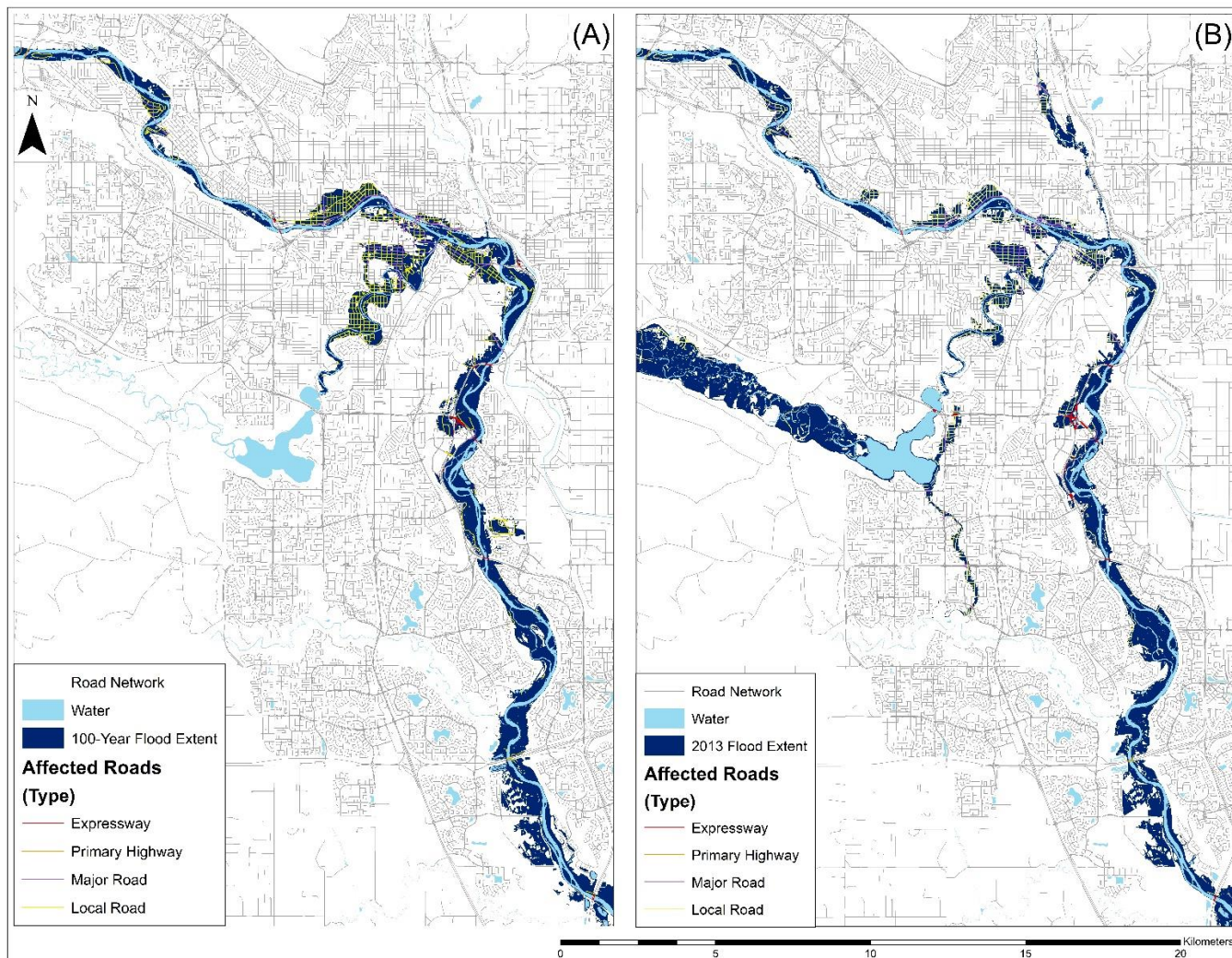


Figure 3. Flood extents and links affected from a (A) 100-year flood and the (B) 2013 flood.

was accomplished by first converting the flood depth raster into a polygon of cells using the Raster to polygon tool. The resulting polygon was then overlaid with the Calgary road network, using the Intersect tool. This tool takes the lowest geometry of the inputs, which is the road network (lines), while maintaining all the attributes of both datasets. Therefore, links in the output appear identical to those in the original Calgary road network shapefile. The resulting flooded road network from the Intersect tool only contained flooded links, where all links have a depth of water greater than zero. The attribute table differed from the Calgary road network as each record was representative of each flood depth cell instead of a link.

The flooded road network should be representative of each link instead of a cell as the network attributes (such as speed and travel time) are characteristic of links. To have each record represent a single link, the data was merged based on the unique identifier (UID). The UID is a unique value used to represent a single link in the road network shapefile. By specifying the statistics, the minimum, maximum, and mean water depth for each link in the road network was obtained when executing the Dissolve tool. A field was added to the flooded road network for each statistic type, then set as the input in the Dissolve Tool. Like the input, the result only contained flooded links and as therefore not the complete road network for Calgary. The flooded network shapefile was joined back to the original Calgary road network in order for the flooded data and road network data to exist in a single shapefile. This was done by executing a join, specifying the join field as the UID for both datasets. These steps were executed twice, once for each of the flood scenarios.

Water depths have been attached to flooded links in the road network, however, the maximum speed and travel times, which is the time in minutes it takes to travel completely along a link, must be updated to reflect the conditions of a flooded road network. To calculate the new maximum speed, the following equation, derived by Pregolato et al. (2017), was used:

$$v(w) = 0.0009w^2 - 0.05529w + 86.9448 \quad (3)$$

A function was fitted to estimate the limit vehicle speed, v , as a function of flood depth, w , which has an R-squared of 0.95 (Pregolato et al., 2017). The speed, $v(w)$, is the maximum acceptable velocity that ensures safe control of the vehicle given the depth of water. By inputting the average depth (millimeters) of water on a link, the new maximum speed was calculated for each link in the network. After the new maximum speed was determined, some values were greater than the speed limit if the depth of water is very low, such as one to five cm. These values must be adjusted so they take the maximum speed limit of the road instead of being the maximum speed of the vehicle. This only applied to links with a flood depth associated with it. For links with a maximum flood depth greater than or equal to 30 cm, they were restricted as cars are not able to navigate safely at this depth. For non-flooded links, travel times and maximum speeds remained the same.

New values and fields were calculated and created in the attribute table of the complete flooded road network shapefile of Calgary. A new restriction field was added, with a value of 1 representing a restricted link. Here, it was assumed that if any point within the link reaches 30 cm, the entire link becomes disabled. Maximum speeds were calculated

following Pregnotato et al.'s (2017) equation. Travel times were then updated based on the new maximum speeds. This was executed for each of the flooding scenarios separately.

5.3. Service Areas

A service area analysis was used to measure the impacts of flooding, in terms of those that cannot be served by emergency services following targeted response times. To execute a service area analysis using ArcGIS, the requirements are: a network dataset, facility locations and an impedance value, which can be in units of time or distance. The network dataset represents the road network and stores the connectivity of features, following topology rules. Facility locations are set to the emergency service locations, which are EMS, fire, and police stations. Since emergency services have targeted response times that must be met, impedance is set to the time of such targets. Service areas are generated following the attributes of the network (e.g., travel time, speed, one ways, and restrictions) to simulate driving conditions. The resulting service area polygons encompass all accessible streets and areas within the specified impedance value.

To measure the changes in accessibility of emergency services during flooding in Calgary, a base case was created. The base case represents the areas and number of people that are served following the various targeted response times, before a flood. Service areas were computed for each emergency service type, resulting with three service area analysis layers. The network dataset was set to the original, non-flooded road network. The facilities were set to the stations of the emergency service being analyzed. The impedance is set to

12 minutes for EMS, 7 and 12 minutes for fire, and 7, 12, 17, 40, and 120 minutes for police.

To compute the service areas for the flooding scenarios, the same parameters were used, other than the network dataset. For the 100-year flood, the network dataset was set to the complete flooded road network derived from predicting the depth of the 100-year flood. For the 2013 flood, the network dataset was set to the complete flooded road network derived from predicting the extent and depth of a four meter flood in Calgary. Overall, service areas were calculated three times for each emergency response type, initially for the base case and the two flood events, resulting with a total of nine service area layers.

For emergency services with multiple time thresholds, such as fire and police, those served within each time threshold are summed together and presented in Tables 1 and 2. The sum of these numbers is equivalent to applying only the maximum time thresholds. The maximum targeted response time is chosen to define those accessible and non-accessible as the analysis reflects flooded conditions, where emergency services will most likely have a greater number of requests compared to non-flooded conditions. Previous reports from residents in Alberta have stated that they waited over two hours for police to arrive following their requests for aid, allowing for the use of the maximum threshold to be appropriate (CTV News, 2019; Mitchell and Romero, 2019). Therefore, the impedance was set to multiple values, where each threshold creates a separate service area polygon based on that value. However, the maps presented do not delineate these boundaries, representing populations served within all thresholds.

Following the targeted response times, there were areas not served even before the event of a flood. To only assess the impacts from those directly related to flooding, those that were not served before the flood were not considered in the analysis. The results presented reflect the changes in accessibility to emergency services. Therefore, areas defined as not served following these flood events were served previous to the events.

5.4. Population

The analysis uses two types of populations: residents and workers. To provide more accurate spatial location of those served and not served by emergency services, residential and work populations, were assigned to only residential and work areas, respectively. This allowed for populations to be mapped at a higher resolution, instead of assuming the population was homogeneously proportioned across the entire subdivision. The population of a residential or commercial area within the subdivision was calculated using the following equation:

$$N_{i,j} = \frac{A_{i,j}}{\sum_{i=1}^I A_{i,j}} \times N_j \quad (4)$$

where $N_{i,j}$ is the population of sub area i in a larger area j . $A_{i,j}$ represents the area of the sub area, while N_j is equal to the total population in the larger area.

Service areas layers for each emergency service type were removed from the base case layer of the corresponding emergency service type, resulting with three outputs for each flood scenario. This was done using the Erase tool, resulting with areas served before the flood event but not after. Areas not served were then overlaid with residential and

commercial land use, separately, using the Intersect tool. Executing this for each emergency service type resulted with a total of six outputs for each flood scenario. These results display residential and commercial area not served within a DA, following targeted response times.

The smallest geographic area for which all census data are disseminated is the DA. The number of residents was calculated for the residential area not served, using Equation 2, where $A_{i,j}$ is the area of the residential polygon not served, the sum of $A_{i,j}$ is equal to the total residential area within the DA, and N_j is the total number of residents in the DA. The same technique was applied to quantify the number of workers not served, where $A_{i,j}$ the area of a commercial polygon not served, the sum of $A_{i,j}$ equal to the total commercial area within the DA, and N_j is the total number of workers in the DA. These results represent the worst case scenario, where the number of residents and workers not served were quantified based on the assumption that populations have not been evacuated in advance of a disastrous flood.

Chapter 6: Results and Discussion

6.1. Population Statistics

6.1.1. EMS

The residential and work populations served by EMS following the 12-minute targeted response time can be seen in Figure 4. 90.12% (1,101,913 residents) of the residential population and 89.58% (589,674 workers) of the work population were accessible as shown in Table 1. In 2016, there were 1,222,735 residents and 658,225 workers in the city of Calgary. Many regions in the outskirts of the city were not served even before the event of a flood. This is caused by the limited number of EMS stations and their central locations, making the 12-minute target response time difficult to meet, even without flooding impedances in the network.

Table 1. Number of residents and workers served before a flood event.

Number of Individuals	EMS	Fire	Police
Residents	1,101,913	1,222,735	1,222,735
Workers	589,674	647,156	658,225

Out of all the emergency service types, EMS represents the greatest non-accessible residential and work populations, as seen in Table 2. The 100-year flood results show 23.12% (283,537 people) of the residential population and 38.47% (253,205 workers) of the work population were not served. Most of the non-accessible population is concentrated in the center-west downtown area, as seen in Figure 5. Due to the area's close proximity to

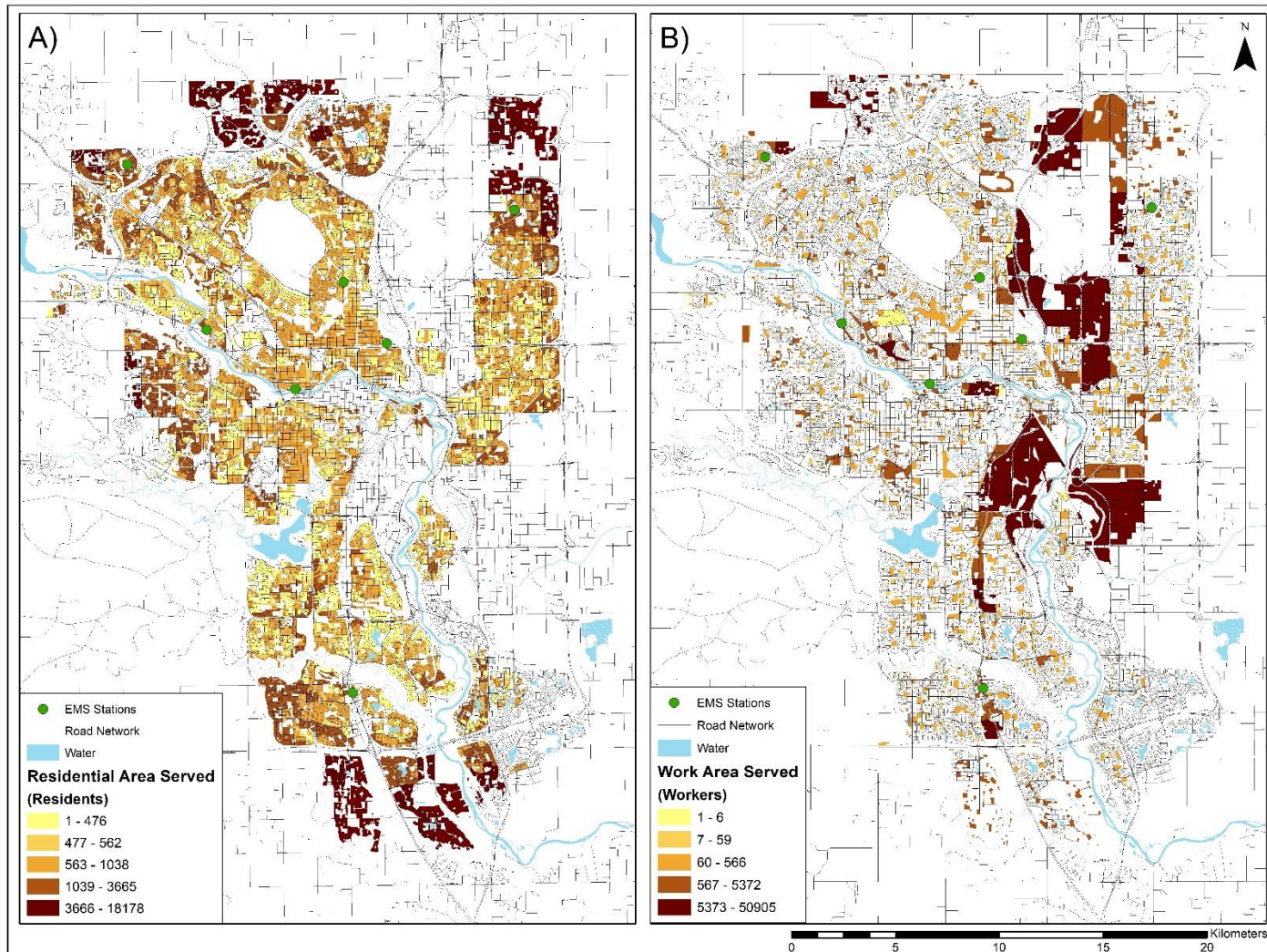


Figure 4. Base case representing (A) residents and (B) workers served by EMS within the 12-minute threshold

the Bow River, many links are flooded (traversable at reduced speeds) and restricted (non-traversable), making it very difficult to reach the residential population. This is also due to the fact that Station #3, located in the center, north of the Bow River, and Station #6, located in the downtown area, south of the Bow River, are located on restricted links. This means that EMS vehicles can no longer be dispatched from these stations. This does not allow the surrounding area to be served as EMS vehicles are now dispatched from farther stations, making it challenging to meet the 12-minute target response time. For this reason, the majority of the areas not served in Figure 5 are found in the downtown center, around the disabled stations. The closest functional station to downtown, south of the Bow River, is Station #15, north of the river. A majority of the links affected by flooding are also located in this area, making the downtown core extremely vulnerable in the event of a 100-year flood. Of the total number of people not served, 4.90% (59,963 people) are 19 or younger and 2.54% (31,063 people) are 65 and over.

Table 2. Residential, dependent and work populations not served.

Number of Individuals	EMS	Fire	Police
<i>100-Year Flood</i>			
Residential Population	283,537	32,863	31,506
0-19	59,963	3,788	3,552
65 and Over	31,063	3,934	3,824
Workers	253,205	34,553	33,009
<i>2013 Flood</i>			
Residential Population	404,425	37,133	36,270
0-19	87,618	5,127	4,957
65 and Over	48,091	5,236	5,081
Workers	309,141	61,117	59,024

Looking at the 2013 flooding event, the numbers are much greater as 33.08% (404,425 people) of the city's residential population and 46.97% (309,141 workers) of the work population are not accessible. Just like the 100-year flood scenario, Station #3 and Station #6 are located on restricted links in the network. Additionally, Station #15 is also on a restricted link, located in the center west, just north of the Bow River. The effects are seen in Figure 6A, with a greater proportion of residential area not being served in the north-west, as well as towards the east side of the city, compared to the 100-year flood. This also reduces the accessibility to workers in the same area, but to a much lesser degree. Figure 6B also shows a greater proportion of the work area being affected, compared to the 100-year flood scenario, which can be observed east of the Bow River and on the north side of the city. This can be attributed to the fact that the 2013 flood had a greater number of restricted links, seen in Table 3. Flooded links are defined by water depths less than 30 cm, allowing for travel. Restricted links represent depths of water 30 cm or greater, preventing travel at any point along the link. Disrupted links represent any links affected by flooding, which is a sum of those restricted and flooded. This results in vehicles being rerouted and increases in travel time, making it more difficult to reach the population within 12-minute threshold. The increase in restricted links is demonstrated in Figure 3, where the 2013 flood has a greater flood extent in the north-east, which is not present in the 100-year flood. This causes cascading effects in the east as greater residential and work populations are no longer accessible within the travel time thresholds. These areas were previously served by Station #4, located in the center east, north of the Bow River, but the larger flood extent intersects routes from the station, severely reducing the number of people from both population types

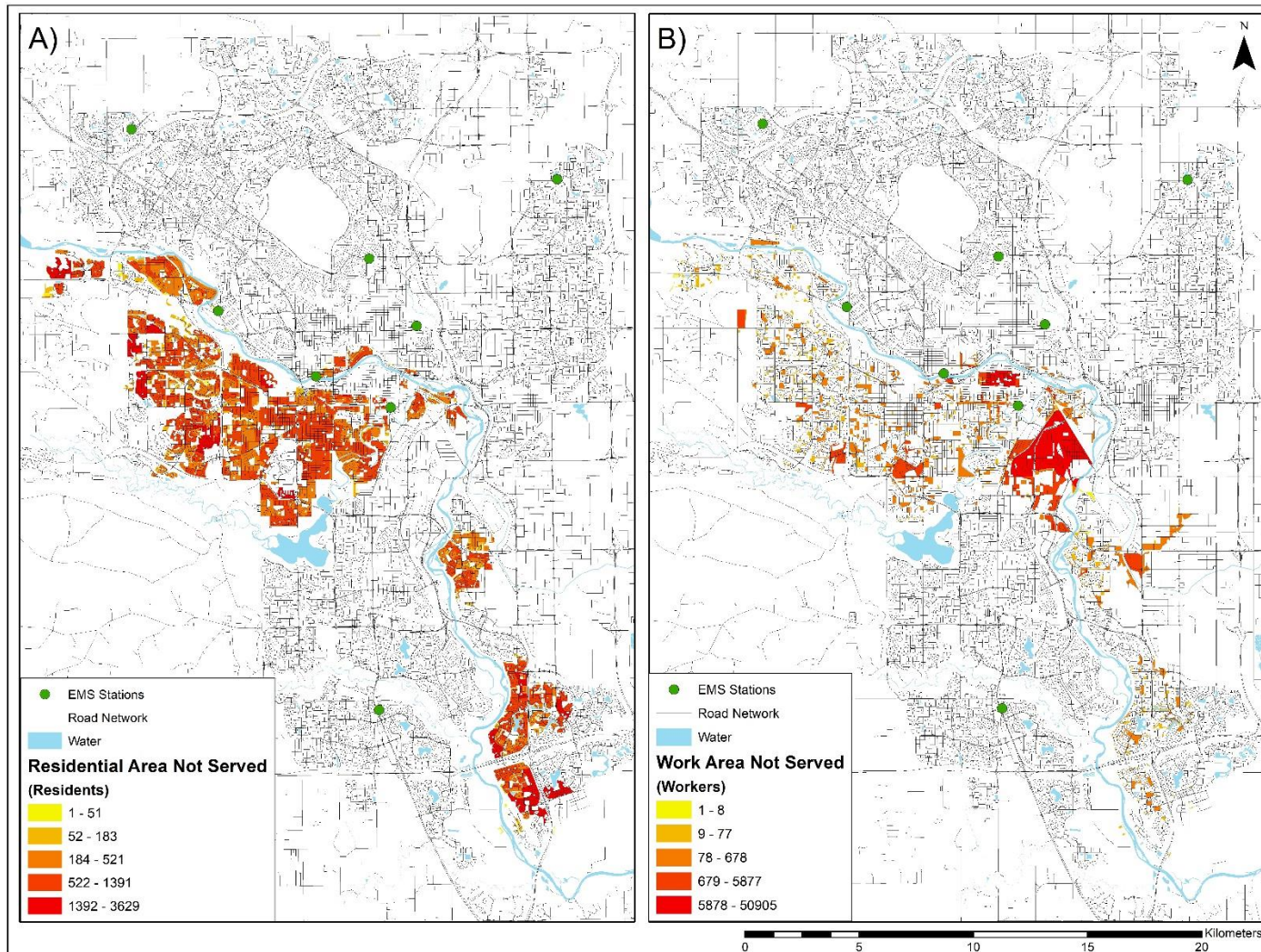


Figure 5. (A) Residents and (B) workers not served by EMS following the 12-minute threshold during a 100-year flood.

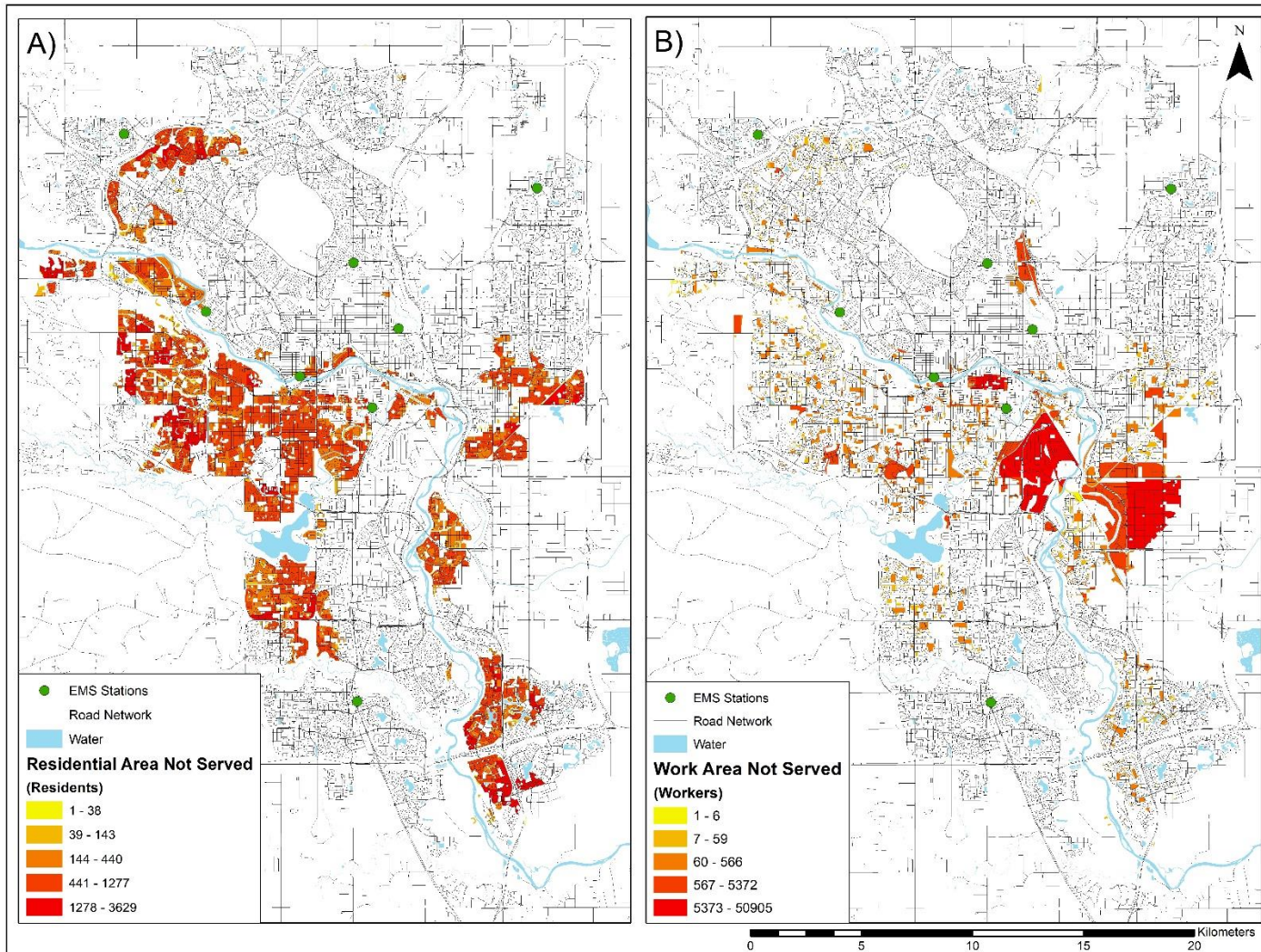


Figure 6. (A) Residents and (B) workers not served by EMS following the 12-minute threshold during the 2013 flood.

to be served. Overall, the larger number of people affected in the 2013 scenario is a combination of the greater number of restricted and flooded links in the network, as well as an additional station not being operational, compared to the 100- year flood scenario. When considering flood mitigation techniques regarding EMS stations, locating a facility east of the Bow River would allow for a greater proportion of both the residential and work population to be accessible during a flooding event.

6.1.2. Fire

Due to the greater number of fire stations and their even distribution across the city, as seen in Figure 7, the entire residential population was served before the event of a flood, seen in Table 1 and Figure 12 in the Appendix. A majority of the work population is accessible within the upper bound of the 12-minute response time as 98.32% (647,156 workers) are be served. The presence of commercial land at the edges of the city has a large influence in the non-accessible population.

Residential areas not accessible to fire services during the 100-year flood can be seen in Figure 7A, corresponding to 2.69% (32,863 people) of the population. These areas are concentrated in the downtown core, adjacent to the Bow River. However, they are in close proximity of multiple stations, meaning that areas not accessible are located on restricted links. Therefore, it is not possible for emergency vehicles to access these locations as they have a depth of water greater than or equal to 30 cm on the link. A majority of the residential area not accessible during the 100-year flood is also not accessible during the 2013 flood, seen in Figure 8A. The slightly larger proportion (3.04%, equating to 37,133 people) of

residents not accessible during the 2013 flood is caused by the greater number of restricted and flooded links, like previously seen with EMS services. The 100-year flood did not have any stations located on restricted links, allowing all 39 fire stations to be functional. However, the 2013 flood had three out of 39 stations located on restricted links, not making them operational in the analysis. Station #1 and Station #6 are located in the downtown core, while Station #9 is located in the east, adjacent to the Bow River. Even with three disabled stations, most of the surrounding areas can still be served as there are other functional stations nearby. In contrast, the effects of disabling EMS facilities caused the immediate surrounding area to not be served, due to the sparse distribution of stations. Figure 8A shows residential areas south of the Glenmore Reservoir that are not accessible, yet they are closely located to two fire stations. This confirms that links in these areas are restricted, caused by 30 cm or greater flood depths. When simulating the 2013 flood extents, mitigation techniques set up by the city were not considered, such as the Glenmore Reservoir. The artificial reservoir controls the downstream flow of the Elbow River, allowing development near the river's bank with less risk of flooding. Thus, the 2013 flood over estimates the number of people not served in these areas as the flood extent is strictly based on the elevation above nearest drainage. Similar conditions are observed in the work population as most parts of the city not accessible during the 100-year flood are also not served during the 2013 flood, with additional areas south of the Glenmore Reservoir. In addition, the 2013 flood has a large, non-accessible area towards the north, representing 977 to 4829 workers. This area is adjacent to a tributary of the Bow River. Since this flooded area does not exist in the 100-year flood extent, there may be flood barriers set up

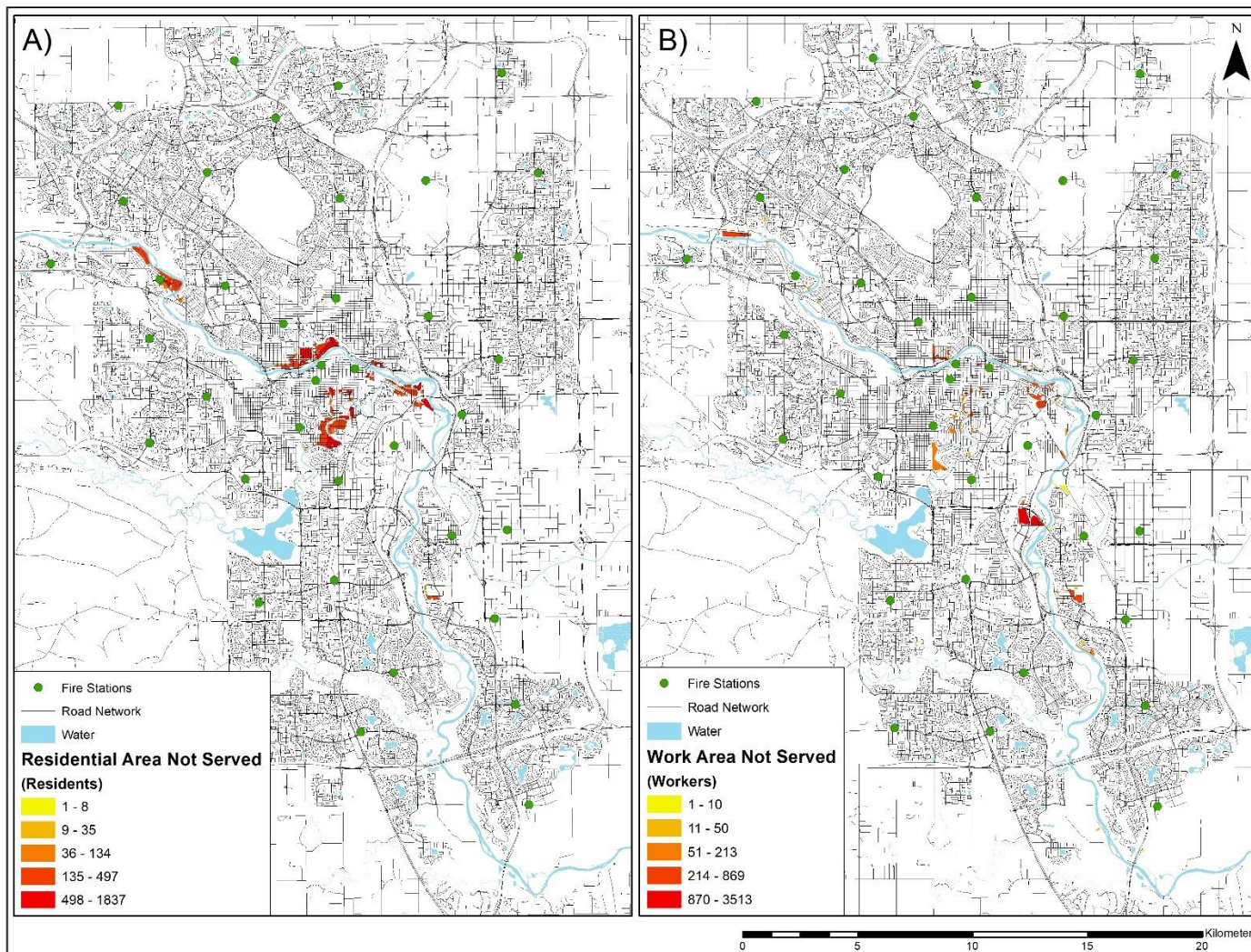


Figure 7. (A) Residents and (B) workers not served by fire following the 12-minute threshold during the 100-year flood.

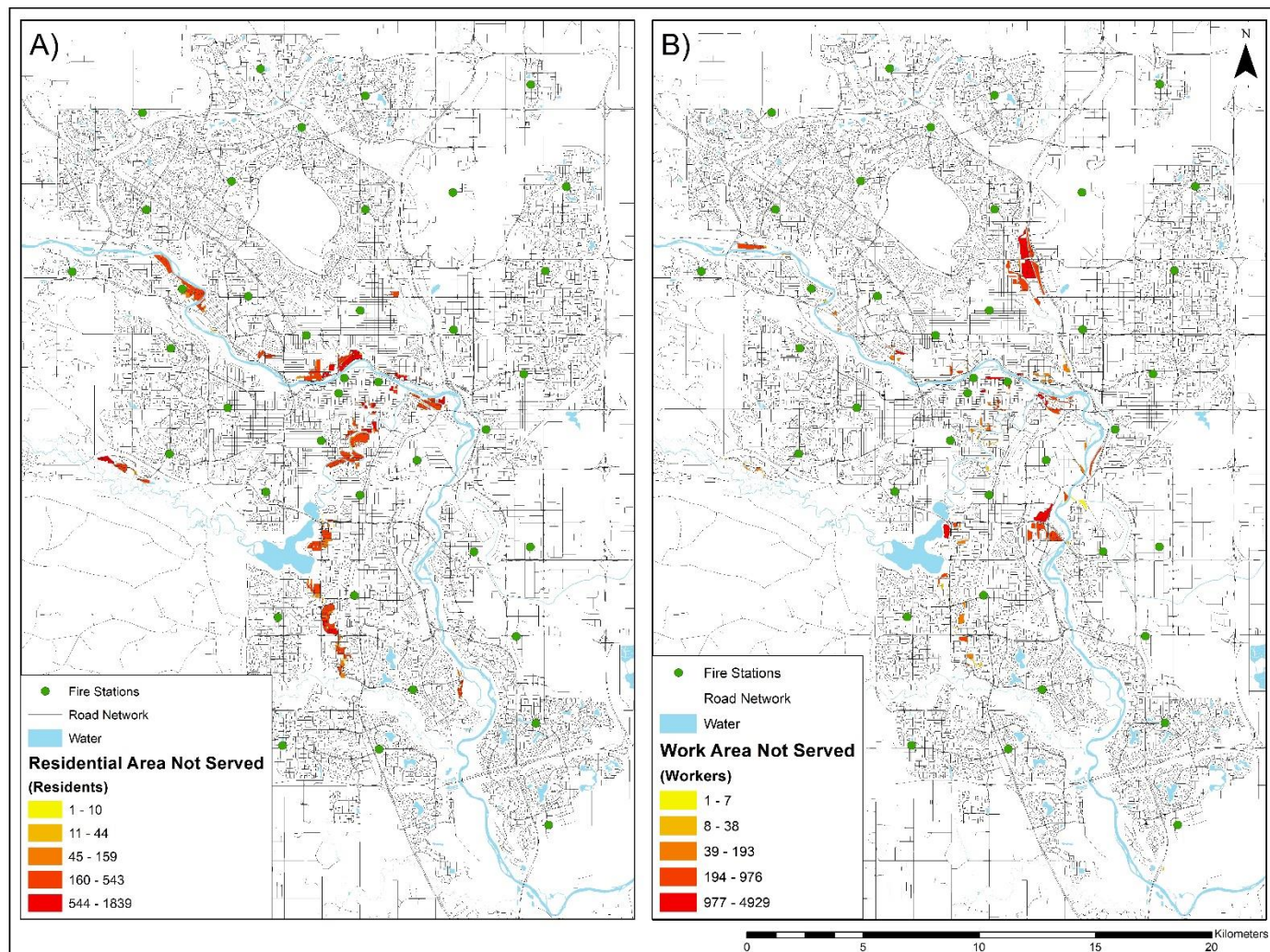


Figure 8. (A) Residents and (B) workers not served by fire following the 12-minute threshold during the 2013 flood.

along the river's banks. These barriers, along with the Glenmore Reservoir, would protect surrounding areas as the quantity and duration of runoff may be reduced, but is not accounted for in the methodology. Overall, response from fire services was shown to be resilient as over 95% of the total population is still accessible during the 100-year flood while over 90% is accessible during the 2013 flood event.

6.1.3. Police

The entire residential and work population was served during the base case, considering the maximum 120-minute response time, displayed in Table 1 and Figure 13 in the Appendix. During the 100-year flood, 2.58% (31,506 people) of the residential population and 5.01% (33,009 workers) of the work population are not accessible from police facilities. Figure 9A shows a majority of the residential area not served being located in the city center, directly adjacent or very close to the Bow River. The consequences of the 2013 flood event results in a larger number of residents (2.97%, 36,270 people) and workers (8.98%, 59,122 workers) not served, as seen in Figure 10. This was also observed previously with both EMS and fire services, which can be explained by a greater number of disrupted links and neglecting mitigation efforts from the city when delineating the 2013 flood extent.

Looking at Table 2, police have the fewest number of residents and workers not served when comparing emergency services types, in both flood scenarios. Police services have a much greater range of response times, which includes up to two hours. Therefore, any areas not accessible by police are located on restricted links, isolating populations, as

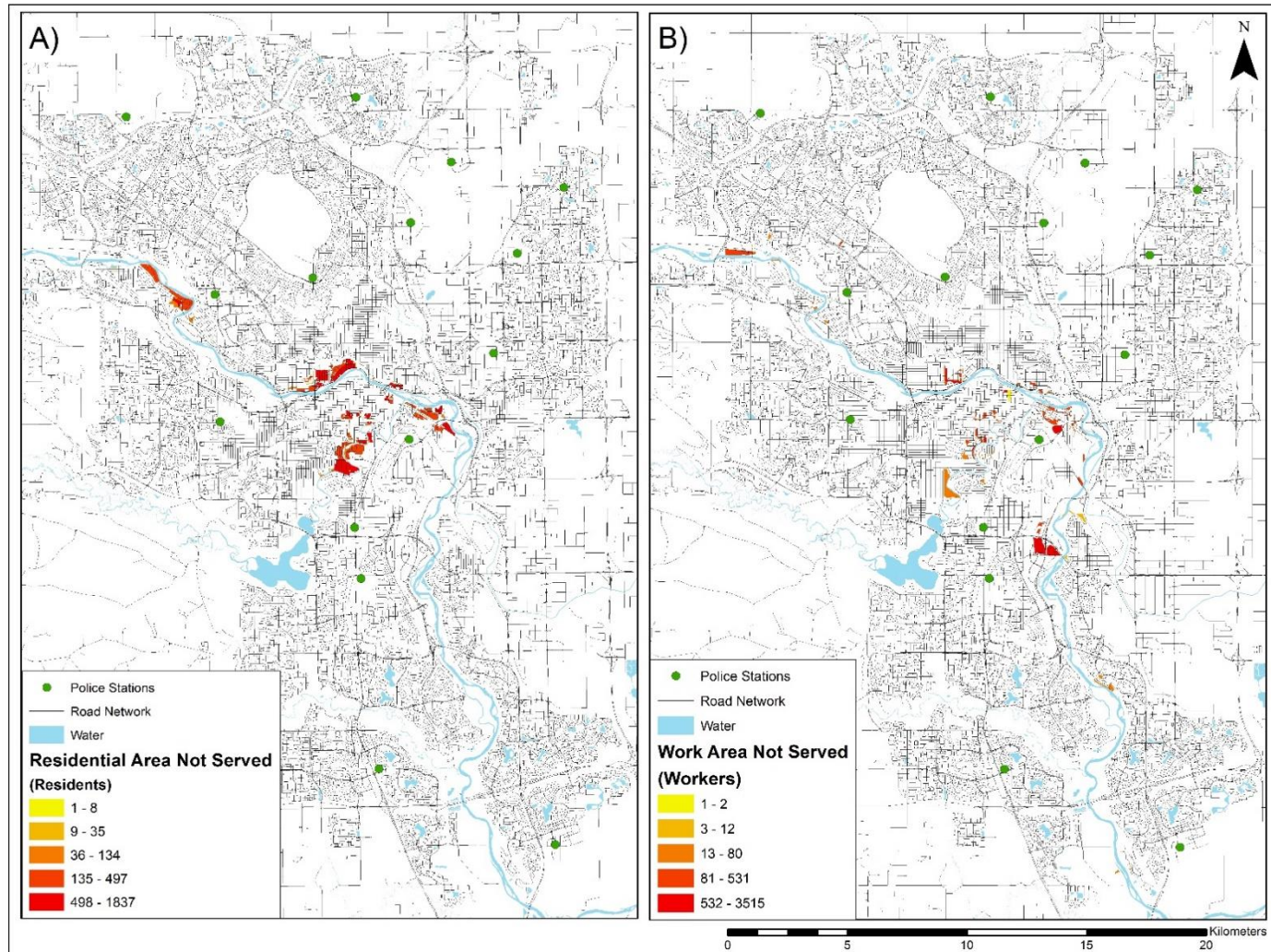


Figure 9. (A) Residents and (B) workers not served by police following the 120-minute threshold during the 100-year flood.

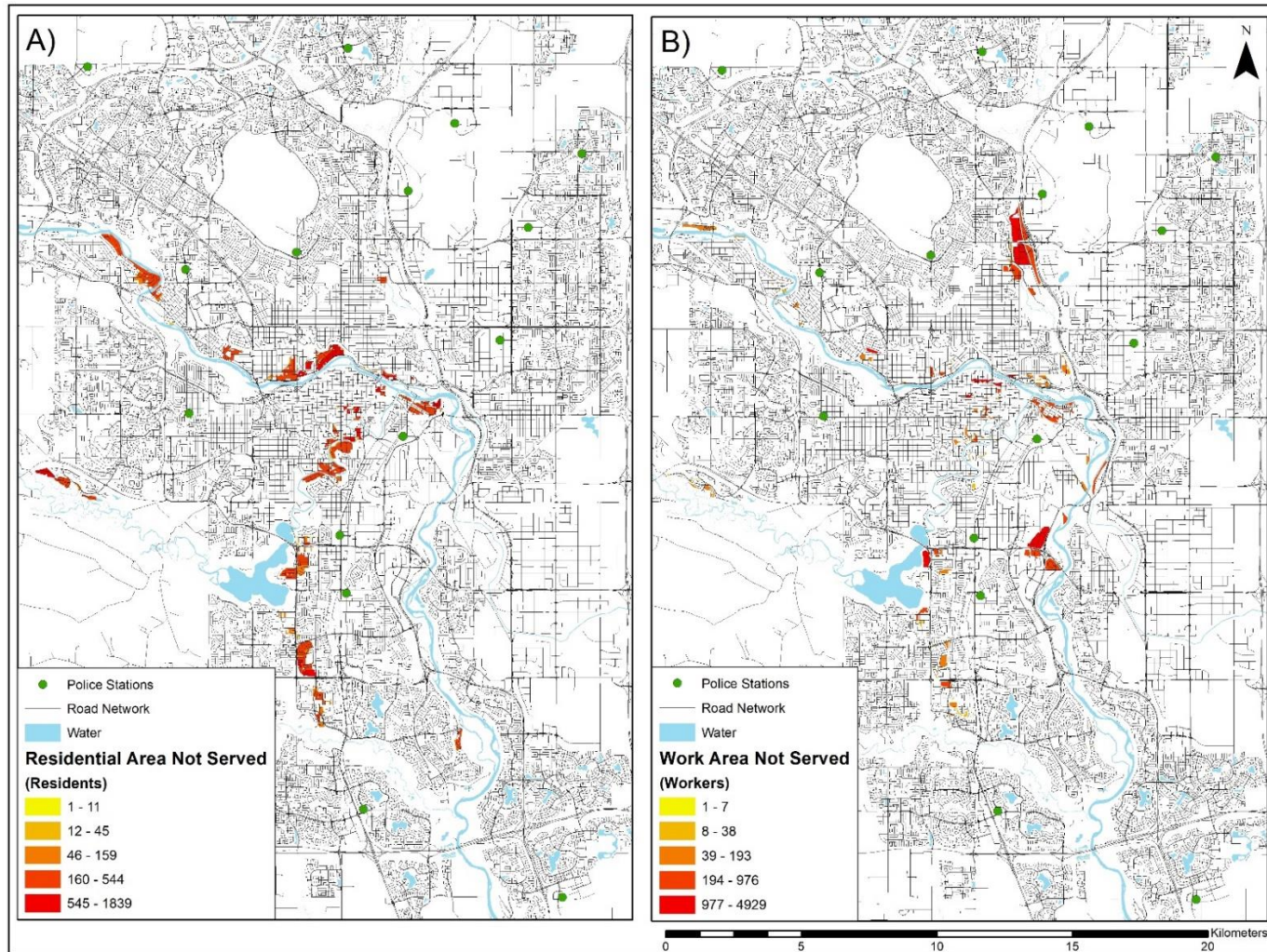


Figure 10. (A) Residents and (B) workers not served by police following the 120-minute threshold during the 2013 flood.

the entire city can be reached within two hours. It is impossible for police services to reach these areas, even with the very minimal time constraints. Since these populations are not accessible strictly due to the conditions of the flooded road network and not the constraints of the response time, they are the most vulnerable as they are not accessible to any emergency service type. The best way to ensure the safety of people living and working in these areas would be to evacuate before the flood reaches a magnitude where the links become restricted.

6.2. Network Statistics

Table 3 displays the number and length of links affected for each flood scenario. Overall, the 2013 flood had a greater disruption of links compared to the 100-year flood. Since the 2013 flood extent encompasses a greater area, it is reasonable that there were a greater number of links affected. The 100-year flood had 1.76% (1467) of the total links in the network affected from flooding, representing 1.03% (204 km) of the total length of the links. The 2013 flood had 2.04% (1694) links affected, representing 1.28% (254 km) of the total length. The 2013 flood has 334 more restricted links, but 107 fewer flooded links compared to the 100-year flood. The mean reduction in speed for the flooded links were 15 km/h, with a standard deviation of 15, for the 100-year flood and 23 km/h, with a standard deviation of 3 for the 2013 flood. Due to the greater number of flooded links during the 100-year flood, there is a much greater range in the reduction in speed compared to the 2013 flood. This supports the proposed methodology as many vehicles can still travel

at slightly reduced speeds within flood extents, providing more realistic driving conditions in the event of a flood.

Table 3. Number and length (km) of links affected during the 100-year and 2013 flood.

	100-Year Flood	2013 Flood
Total Number of Links	83,241	83,241
Total Length of Links (km)	19,909	19,909
Links Not Flooded	81,774	81,547
Length of Links Not Flooded (km)	19,705	19,655
Number of Links Disrupted	1,467	1,694
Length of Links Disrupted (km)	204	254
Number of Flooded Links	111	4
Length of Flooded Links (km)	14	1
Number of Restricted Links	1,356	1,690
Length of Restricted Links (km)	190	215

Ultimately, the greater number of restricted links during the 2013 flood caused more severe consequences as there was a greater number of individuals not accessible to emergency services, compared to the 100-year flood event. In the event of a disaster, the population will likely be rescued in a reasonable time frame, but not meet the predefined goals. The greater number of restricted links during the 2013 flood may lead to more serious consequences as populations or emergency service facilities will become isolated.

Table 4 displays the number and length of each type of link affected. In all instances, the 2013 flood had a greater number of links disrupted. During both the 2013 and the 100-year flood scenarios, local roads had the greatest number of links affected, followed by major roads and expressways. The number of links disrupted compared to the total number of links in each of the five classes all fall below 5%. When looking at the relative proportion

Table 4. Number and length (km) of each type of link affected.

	Expressway	Primary Highway	Secondary Highway	Major Road	Local Road
<i>100-Year</i>					
Total Links	1,649	2,564	1,514	6,900	70,614
Total Length (km)	618	1,196	1,009	1,062	16,029
Links Not Flooded	1,586	2,552	1,514	6,627	69,495
Length of Links Not Flooded (km)	599	1,194	1,008	1,018	15,886
Number of Links Disrupted	63	12	0	273	1,119
Length of Links Disrupted (km)	20	2	0	4	140
Number of Flooded Links	11	1	0	28	71
Length of Flooded Links (km)	3	0	0	4	8
Number of Restricted Links	52	11	0	245	1048
Length of Restricted Links (km)	17	2	0	40	132
<i>2013</i>					
Total Links	1,649	2,564	1,514	6,900	70,614
Total Length (km)	618	1,196	1,009	1,062	16,029
Links Not Flooded	1,578	2,543	1,514	6,594	69,318
Length of Links Not Flooded (km)	597	1,189	1,008	1,012	15,846
Number of Links Disrupted	71	21	0	306	1,292
Length of Links Disrupted (km)	21	6	0	50	177
Number of Flooded Links	0	0	0	0	5
Length of Flooded Links (km)	0	0	0	0	1
Number of Restricted Links	71	21	0	306	1292
Length of Restricted Links (km)	21	6	0	50	176

of each link type affected, major roads was the most affected, followed closely by expressways. This is important as expressways have higher speed limits and capacities, making them crucial in reaching the population in a timely matter. However, speed is not a major factor here as emergency service vehicles do not have to obey speed limits. Therefore, the bigger concern here are the number and length of links that become restricted, meaning vehicles can no longer traverse them, leaving populations isolated. Similar to the largest number and length of links disrupted, the highest restriction comes

from local roads, followed by major roads and expressways. Local roads are also more likely to become congested due to their smaller capacity, compared to expressways. Therefore, when observing the non-accessible populations, those located on restricted, local roads are the most vulnerable. Quantifying and locating restricted roads in the network can help municipalities decide where to add new flood barriers or prioritize the removal of flood water on the road. These strategies can mitigate or help adapt to the impacts of flooding such that emergency services can provide efficient rescue and response.

6.3. Research Contributions

6.3.1. Accessibility Modelling

Despite the extensive field of accessibility modelling, there is limited research that models the response of emergency services, while accounting for the partial degradation of the road network. Previous studies have analyzed flooding on the network, acknowledging the relationship between water depth and vehicle speed (Pregolato et al., 2017) and the accessibility of emergency services (Coles et al., 2017; Green et al., 2017; Albano et al., 2014; Indriasari et al., 2010), but the two have yet to be examined together. By accounting for flooded links in the network, travel times, maximum speeds, and the functionality of road links were modelled more realistically and provide better insight to the consequences of flooding on the population, demonstrated for the city of Calgary.

This research contributes to studies modelling the accessibility of emergency services, where previous authors modelled inundated roads as binary (Suarez et al., 2005; Coles et al., 2017; Green et al., 2017). To demonstrate the improvements of using this

model, additional scenarios were developed following this assumption. Service areas were simulated on a flooded network where all links falling within the flood extent were considered restricted. The number of non-accessible people and workers were quantified, applying the same techniques in distributing populations. The non-accessible population following the methodology introduced in this paper was subtracted from the non-accessible population calculated from restricting travel on all disrupted links, presented in Table 5. As predicted, restricting all links within flood extents estimated a larger population not accessible by emergency services as a greater number of links were no longer traversable. When comparing the flood scenarios, the 2013 flood event overestimated the number of non-accessible residents and workers in all instances other than residents served by fire services. It should be expected that this holds true for all emergency service types and populations as the methods introduced in this study to estimate those not served during the 2013 flood also overestimate reality as flood barriers set up by the city were not considered. Therefore, as the 100-year flood not only considers barriers and dams but also hydrologic conditions of the area when delineating the flood extent, these results provide the most accurate prediction in determining the non-accessible population. By permitting travel on a degraded network, routes and service areas were simulated to reflect more realistic flood conditions. These results contribute to emergency planning as it allows for vulnerable populations to be quantified and located. Following the steps in the base case would overestimate those who are in need during disaster. The results presented in this study can help allocate resources where they are crucially needed most and ensure services are available to those that are in the most danger.

Table 5. Overestimation of non-accessible individuals following the base case conditions.

Number of Individuals	EMS	Fire	Police
<i>100-Year Flood</i>			
Total Population	7,086	8,468	4,152
0-19	1,373	1,264	392
65 and Over	931	765	213
Workers	6,329	29,250	26,015
<i>2013 Flood</i>			
Total Population	3,607	9,714	386
0-19	795	1,716	152
65 and Over	477	1,925	246
Workers	3,387	16,966	53,915

6.3.2. Flood Inundation Mapping

The methodology introduced to create flood depth maps uses the capabilities of GIS, with the limited availability of open source data. Despite not considering hydrodynamic data (such as flow velocity), the flooded areas in the 100-year and 2013 flood events showed comparable extents, recognizing the prediction skills of this simple and fast method. The recent advancements in spatial modelling software and terrain descriptors allows for the development of inundation mapping techniques with simplified input requirements (Renno et al., 2008; Elshorbagy et al., 2017; Afshari et al., 2018; Schnebele et al., 2014). Such techniques are preferred compared to those requiring extensive data, comprehensive hydrologic models and complex computation, especially in emergency response scenarios where time is limited.

The 2013 flood extent data mapped by the city of Calgary could be used following the same methods as the 100-year flood to derive flood depths, but was used in this study

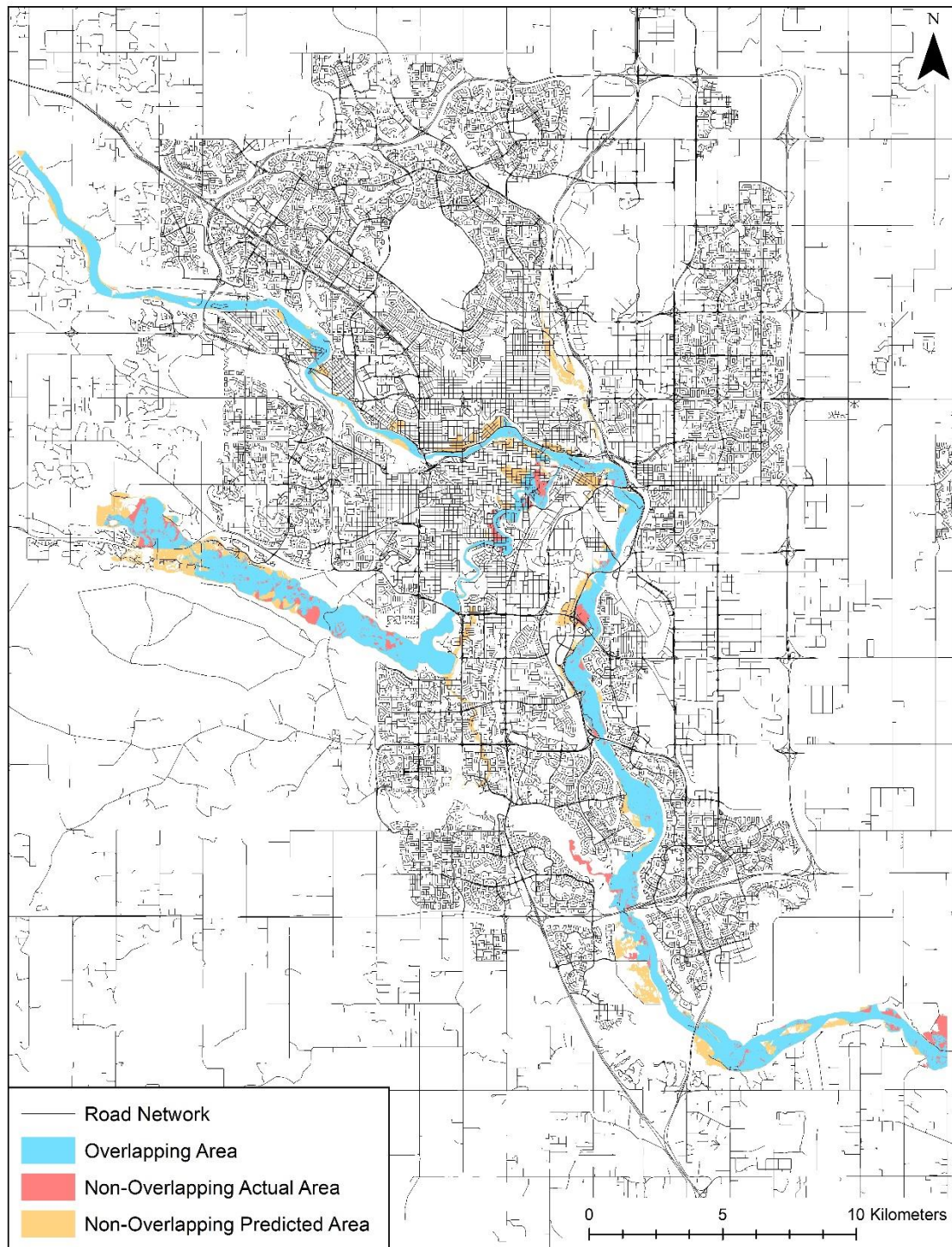


Figure 11. Validation of 2013 flood extent by comparing overlap of reference data.

as reference data to verify the approach developed in delineating the 2013 flood. The 2013 flood extent mapped in this study was overlaid with the flood extent mapped by the city of Calgary, as seen in Figure 11. The extent mapped by the city had an area of 46 square kilometers (km^2), while the extent mapped here had a total of 56 km^2 . The non-overlapping actual area represented the flood extent mapped by the City that does not overlay the flood extent mapped in this study, while the non-overlapping predicted area represented the flood extent mapped using the proposed methodology but was not part of the flood extent by the city. However, as previously mentioned, the flood extent mapped by the City was based on an aerial photo from June 22, 2013, taken after the peak has passed. Hydrologic data from Environment Canada showed the peak water level occurring on June 21, 2019, which was used in this study. Therefore, it is reasonable that the flood extent derived using the methodology introduced here was greater than the reference extent. The 88% (40.84 km^2) of overlapping area suggests that the methodology is suitable for rapid flood inundation mapping at the city-scale level.

Chapter 7: Summary and Conclusion

7.1. Summary of Findings

This study evaluated the accessibility of emergency services by integrating flood inundation mapping with network analysis. The consequences of two flooding events were observed in Calgary, Alberta, displaying the total residential and work population no longer accessible following the targeted response times of EMS, fire, and police services. The residential population could be further classified to reflect the dependent population, those under 19 and over 65 years of age. By quantifying and locating the number of individuals not served, the results identify vulnerable areas in the city. In addition, the research identifies vulnerable links in the network, based on the reduction of vehicle speed and restriction of travel. The methods introduced in this study have much wider applications than the city of Calgary, allowing for quick analysis of emergency response in the event of a disaster.

Comparing the residential population to the work population, all services, other than EMS, in both flood scenarios had a greater number of workers not accessible. This was likely due to the fact that the distribution of workers was more concentrated compared to residents, so even if a small commercial area was located on a restricted link, a larger population than expected may be affected. The opposite effects could be seen when looking at EMS services for both flood scenarios as a greater residential population was not accessible. The time constraint of 12 minutes played a large role in the number of people that could not be served as the sparse location of emergency facilities caused vehicles to travel much greater distances in order to serve residents. A large proportion of the

population also resides towards the city boundary as the land use of these neighborhoods is typically residential, furthering the difficulty in meeting the time constraint. Unlike EMS, those not accessible by fire and police were more centrally located and closer to the rivers. These two services were limited by the restriction of links instead of the time constraint. Overall, EMS showed the greatest reduction in accessibility, caused by the smaller number of stations compared to fire and police services. EMS are trained to provide acute care to life threatening issues and are responsible for transporting individuals to hospitals, making the accessibility of this service very crucial to the health and safety of the population. Even though fire services have the same maximum time threshold of 12 minutes, the number of individuals not accessible was much smaller due to the number of stations and their distribution across the city. Therefore, locating additional facilities and distributing them evenly across the city will allow for EMS to remain resilient, similar to fire services, which still had access to over 90% of the work and residential population.

Despite the technology and models available to predict flooding events, they might not provide an accurate estimation during an emerging and unpredictable disaster. The consequences are magnified due to the concentration of populations in megacities, placing more people at risk (Hooke, 2000). A common mitigation technique executed by municipalities is evacuating populations at risk, as seen during the 2013 Alberta flood in Calgary. The timing and type of evacuation (mandatory, recommended, and voluntary) will affect emergency vehicles and equipment access to the emergency areas depending on the number of people who choose to evacuate (Alsnih and Stopher, 2004). The results presented determined those not accessible by emergency services, but can also aid in

deciding where and when populations should be evacuated. The analysis defined vulnerable populations as those without access to emergency services, where the most vulnerable populations were defined by those without access to all EMS, fire, and police. These populations should face mandatory evacuation as they are located on restricted links in the network, possibly leaving them isolated. To determine when populations should be evacuated, the historic flood mapping technique can be executed for different flood heights, for example one to three meters. The accessibility of emergency services can then be quantified at different stages of a flood, determining the proportion of the population not served and the increases between stages. Therefore, the methods introduced for flood depth mapping aid in decision making for municipalities, providing early warning and evacuation strategies to flooding events.

7.2. Limitations

This research used the equation derived by Pregnolato et al. (2017) to model vehicle speed, which had uncertainties from other factors unrelated to flood depth, such as tire pressure, road pavement, and behavior of driver or visibility. Also, a threshold of 30 cm was used to define restricted links, which is commonly agreed upon for passenger vehicles. However, emergency vehicles, especially fire trucks, have greater weights, tire size and height above the ground, allowing them to travel at greater depths of water before becoming buoyant. Considering characteristics of emergency service vehicles could likely result in fewer restricted links in the network as the threshold would be greater. As a consequence, service areas may change significantly, as a greater number of people and workers could

be served within the targeted response times. Stations located on restricted links in this analysis may also become operational with a change in threshold. This would have a considerable effect on EMS during the 100-year flood as two of the eight stations could not dispatch vehicles. Additionally, this would affect both EMS and fire services during the 2013 flood, as three EMS stations and three fire stations were located on restricted links. Refining the equation to account for characteristics of vehicles will allow for a greater range of applications.

This analysis determined whether emergency service vehicles could meet targeted response times during a flood. Service areas generated were based on travel times from dispatch stations, following the maximum speed of links. However, emergency vehicles are not required to follow speed limits, allowing them to reach their destinations in a shorter amount of time compared to standard vehicles. Accounting for this would result with a smaller population not being served. The effects would be pronounced with EMS and the residential population as those not served were mainly due to the time constraint, instead of being located on a restricted link. Also, many emergency response vehicles have real-time GPS devices attached, which allow them to respond to emergencies in the most efficient way. Vehicles may not necessarily be dispatched from a station, but instead from their current position, possibly reaching the population faster than they are expected to. An additional limitation that would affect the response time of emergency services was not accounting for traffic congestion. When service areas were simulated for the flood events, the road capacity remained the same, which assumed the same number of vehicles were

passing through the link. Real-time data would give more realistic estimates of service areas as they depend on traffic conditions.

Despite the advantages of the introduced methods, they are limited to fluvial flooding events. Future research exploring the drainage systems of a city could allow for the analysis to be applied to pluvial floods as well. Urban drainage systems are infrastructure designed to remove excess rainfall and ground water from impervious surfaces. However, when drainage systems are exceeded or fail, flood waters can interact with runoff from water courses and rivers. Increases in urban development coupled with increased pluvial floods due to climate change may magnify the risk of flooding to populations who are already vulnerable to fluvial floods. By considering the drainage of a city and the spatial and temporal rainfall patterns, inundation maps can also be generated from pluvial events, allowing for flood depth maps to be created for either type of flooding event.

7.3. Concluding Remarks

Understanding the consequences of flooding aids decision makers regarding land use plans, emergency response strategies, infrastructure design, and policy planning to improve the safety and future development of cities. Modelling the performance of the network under flooded conditions is essential for mitigating the consequences for future, unpredicted events. This study identified vulnerable populations based on the accessibility of emergency services, accounting for partially flooded links in the network. Many of the limitations in this study were caused by the availability of data. However, the introduction of less complex methods for inundation mapping, allows for rapid analysis, which can be

easily applied to different study areas. The results can be used to increase the resilience of cities to flooding through emergency management plans and the design of flood protection infrastructure. We have no control over the occurrence of extreme events, but by focusing on effective urban planning, optimal solutions can be executed to reduce and avoid impacts. To improve on the methods introduced in this study, future investigation should consider the characteristics of emergency vehicles, such as height, weight, and tire size. This may allow for travel on flooded links with depths greater than 30 cm, or a reduction in speed at a much lesser degree, enhancing prevention and response capabilities during flooding disasters.

References

- Afshari, S., Tavakoly, A., Rajib, M., Zheng, X., Follum, M., Omranian, E. and Fekete, B. (2018). Comparison of new generation low-complexity flood inundation mapping tools with a hydrodynamic model. *Journal of Hydrology*, 556, 539-556.
- Albano, R., Sole, A., Adamowski, J., and Mancusi, L. (2014). A GIS-based model to estimate flood consequences and the degree of accessibility and operability of strategic emergency response structures in urban areas. *Natural Hazards and Earth System Sciences*, 14, 2847-2865.
- Alsnihi, R., and Stopher, P. (2004). Review of procedures associated with devising emergency evacuation plans. *Transportation Research Record: Journal of the Transportation Research Board*, 1865, 89-97.
- AMAP (2011). Arctic Climate Issues 2011: Changes in Arctic Snow, Water, Ice and Permafrost. *Arctic Monitoring and Assessment Programme*. Available at: <https://www.amap.no/documents/doc/arctic-climate-issues-2011-changes-in-arctic-snow-water-ice-and-permafrost/129> [Accessed September 3, 2019].
- Arampatzis, G., Kiranoudis, C., Scaloubacas, P., and Assimacopoulos, D. (2004). A GIS-based decision support system for planning urban transportation policies. *European Journal of Operational Research*, 152, 465-475.
- Balica, S., Wright, N., and van der Meulen, F. (2012). A flood vulnerability index for coastal cities and its use in assessing climate change impacts. *Natural Hazards*, 64, 73-105.
- Balijepalli, C., and Oppong, O. (2014). Measuring vulnerability of road network considering the extent of serviceability of critical road links in urban areas. *Journal of Transport Geography*, 39, 145-155.
- Berdica, K. (2002). An introduction to road vulnerability: what has been done is done and should be done. *Transport Policy*, 10, 81.

- Bono, F., and Gutiérrez, E. (2011). A network-based analysis of the impact of structural damage on urban accessibility following a disaster: the case of the seismically damaged Port Au Prince and Carrefour urban road networks. *Journal of Transport Geography*, 19, 1443-1455.
- Brivio, P., Colombo, R., Maggi, M., and Tomasoni, R. (2002). Integration of remote sensing data and GIS for accurate mapping of flooded areas. *International Journal of Remote Sensing*, 23, 429-441.
- Brody, S., Zahran, S., Maghelal, P., Grover, H., and Highfield, W. (2007). The rising costs of floods: examining the impact of planning and development decisions on property damage in Florida. *Journal of the American Planning Association*, 73, 330-345.
- Burton, I. (2015). Floods in Canada. *The Canadian Encyclopedia*. Available at: <https://www.thecanadianencyclopedia.ca/en/article/floods-and-flood-control> [Accessed April 17, 2019].
- Calgary Herald (2013). Timeline: How the great flood of 2013 evolved. *Calgary Herald*. Available at: <https://calgaryherald.com/news/local-news/timeline-how-the-great-flood-of-2013-evolved> [Accessed May 17, 2019].
- Chakraborty, J., Tobin, G., and Montz, B. (2005). Population evacuation: assessing spatial variability in geophysical risk and social vulnerability to natural hazards. *Natural Hazards Review*, 6, 23-33.
- Chang, S. (2010). Urban disaster recovery: a measurement framework and its application to the 1995 Kobe earthquake. *Disasters*, 34, 303-327.
- Chang, S., and Nojima, N. (2001). Measuring post-disaster transportation system performance: the 1995 Kobe earthquake in comparative perspective. *Transportation Research Part A: Policy and Practice*, 35, 475-494.
- Chen, X., Meaker, J., and Zhan F. (2006). Agent-based modeling and analysis of hurricane evacuation procedures for the Florida Keys. *Natural Hazards*, 38, 321-338.

- Chen, X., Lu, Q., Peng, Z., and Ash, J. (2015). Analysis of transportation network vulnerability under flooding disasters. *Transportation Research Record: Journal of the Transportation Research Board*, 2532, 37-44.
- Cho, S., Gordon, P., Moore II, J., Richardson, H., Shinozuka, M., and Chang, S. (2001). Integrating transportation network and regional economic models to estimate the costs of a large urban earthquake. *Journal of Regional Science*, 41, 39-65.
- Church, R., and Cova, T. (2000). Mapping evacuation risk on transportation networks using a spatial optimization model. *Transportation Research Part C: Emerging Technologies*, 8, 321-336.
- City of Calgary (2018a). Flooding in Calgary: Understanding flooding. *Calgary*. Available at: <http://www.calgary.ca/UEP/Water/Pages/Flood-Info/Types-of-flooding-in-Calgary/Understand-Flooding.aspx> [Accessed April 17, 2019].
- City of Calgary (2018b). The flood of 2013. *Calgary*. Available at: <http://www.calgary.ca/UEP/Water/Pages/Flood-Info/Flooding-History-Calgary.aspx> [Accessed April 17, 2019].
- City of Calgary (2018c). Flood Extents from June 22, 2013. *Calgary*. Available at: <https://data.calgary.ca/Environment/Flood-extents-from-June-22-2013/sqfh-d2dp> [Accessed June 18, 2019].
- Coles, D., Yu, D., Wilby, R., Green, D. and Herring, Z. (2017). Beyond ‘flood hotspots’: modelling emergency service accessibility during flooding in York, UK. *Journal of Hydrology*, 546, 419-436.
- CTV News (2019). EPS struggling to meet response time goals. *CTV News Edmonton*. Available at: <https://edmonton.ctvnews.ca/eps-struggling-to-meet-response-time-goals-1.4307766> [Accessed April 17, 2019].

- D'Este, G.M., and Taylor, M.A.P. (2001). Modelling network vulnerability at the level of the national strategic transport network. *Journal of the Eastern Asia Society for Transportation Studies*, 4, 1–14.
- Dimopoulou, M., and Giannikos, I. (2004). Towards an integrated framework for forest fire control. *European Journal of Operational Research*, 152, 476-486.
- Dippel, S. (2018). Calgary council upholds 7-minute fire response time target. *CBC*. Available at: <https://www.cbc.ca/news/canada/calgary/calgary-fire-response-time-council-vote-1.4585135> [Accessed May 17, 2019].
- Elshorbagy, A., Bharath, R., Lakhanpal, A., Ceola, S., Montanari, A., and Lindenschmidt, K. (2017). Topography- and nightlight-based national flood risk assessment in Canada. *Hydrology and Earth System Sciences*, 21, 2219-2232.
- Environment and Climate Change Canada. (2017). Canada's top ten weather stories of 2013. *Government of Canada*. Available at: <http://ec.gc.ca/meteowweather/default.asp?lang=En&n=5BA5EAF-1&offset=2&toc=hide> [Accessed May 17, 2019].
- Erath, A., Birdsall, J., Axhausen, K., and Hajdin, R. (2009). Vulnerability assessment methodology for Swiss road network. *Transportation Research Record: Journal of the Transportation Research Board*, 2137, 118-126.
- Fischer, M. (2006). *Spatial Analysis and GeoComputation*. Heidelberg: Springer Berlin · Heidelberg.
- Fletcher, R. (2018). Calgary faces 3.9% chance of '1-in-100-year' flood before major mitigation is built. *CBC News*. Available at: <https://www.cbc.ca/news/canada/calgary/calgary-flood-elbow-river-mitigation-five-year-anniversary-1.4702742> [Accessed September 3, 2019].

- Geurs, K. and van Wee, B. (2004). Accessibility evaluation of land-use and transport strategies: review and research directions. *Journal of Transport Geography* 12, 127-140.
- Green, D., Yu, D., Pattison, I., Wilby, R., Boshier, L., Patel, R., Thompson, P., Trowell, K., Draycon, J., Halse, M., Yang, L. and Ryley, T. (2017). City-scale accessibility of emergency responders operating during flood events. *Natural Hazards and Earth System Sciences*, 17, 1-16.
- Government of Canada (2019). Daily Water Level Data for BOW RIVER AT CALGARY (05BH004). *Government of Canada*. Available at: https://wateroffice.ec.gc.ca/search/historical_e.html [Accessed April 17, 2019].
- Hall, J., Dawson, R., Sayers, P., Rosu, C., Chatterton, J. and Deakin, R. (2003). A methodology for national-scale flood risk assessment. *Maritime Engineering*, 156, 235-247.
- Hammond, M., Chen, A., Djordjević, S., Butler, D., and Mark, O. (2013). Urban flood impact assessment: A state-of-the-art review. *Urban Water Journal*, 12, 14-29.
- Hansen, W. (1959). How accessibility shapes land use. *Journal of the American Institute of Planners*, 25, 73-76.
- Hirabayashi, Y., Mahendran, R., Koirala, S., Konoshima, L., Yamazaki, D., and Watanabe, S. (2013). Global flood risk under climate change. *Nature Climate Change*, 3, 816-821.
- Holmes, K., Chadwick, O. and Kyriakidis, P. (2000). Error in a USGS 30-meter digital elevation model and its impact on terrain modeling. *Journal of Hydrology*, 233, 154-173.
- Hooke, W. (2000). U.S. Participation in international decade for natural disaster reduction. *Natural Hazards Review*, 1, 2-9.

- Horner, M., and Widener, M. (2011). The effects of transportation network failure on people's accessibility to hurricane disaster relief goods: a modeling approach and application to a Florida case study. *Natural Hazards*, 59, 1619-1634.
- Houston, D. (2011). Pluvial (rain-related) flooding in urban areas: the invisible hazard. *Joseph Rowntree Foundation*. Available at: <https://www.jrf.org.uk/report/pluvial-rain-related-flooding-urban-areas-invisible-hazard> [Accessed August 7, 2019].
- Indriasari, V., Mahmud, A., Ahmad, N., and Shariff, A. (2010). Maximal service area problem for optimal siting of emergency facilities. *International Journal of Geographical Information Science*, 24, 213-230.
- IPCC (2014). Near-term Climate Change: Projections and Predictability. *Intergovernmental Panel on Climate Change*. Available at: https://www.ipcc.ch/site/assets/uploads/2018/02/WG1AR5_Chapter11_FINAL.pdf [Accessed September 3, 2019].
- Jafarzadegan, K., and Merwade, V. (2019). Probabilistic floodplain mapping using HAND-based statistical approach. *Geomorphology*, 324, 48-61.
- Jenelius, E., and Mattsson, L. (2015). Road network vulnerability analysis: conceptualization, implementation and application. *Computers, Environment and Urban Systems*, 49, 136-147.
- Jenelius, E., Petersen, T., and Mattsson, L. (2006). Importance and exposure in road network vulnerability analysis. *Transportation Research Part A: Policy and Practice*, 40, 537-560.
- Jongman, B., Kreibich, H., Apel, H., Barredo, J., Bates, P., Feyen, L., Gericke, A., Neal, J., Aerts, J., and Ward, P. (2012). Comparative flood damage model assessment: towards a European approach. *Natural Hazards and Earth System Sciences*, 12, 3733-3752.

- Jonkman, S., Maaskant, B., Boyd, E., and Levitan, M. (2009). Loss of life caused by the flooding of New Orleans after hurricane Katrina: Analysis of the Relationship between Flood Characteristics and Mortality. *Risk Analysis*, 29, 676-698.
- Karmakar, S., Simonovic, S., Peck, A., and Black, J. (2010). An information system for risk-vulnerability assessment to flood. *Journal of Geographic Information System*, 2, 129-146.
- Kasperson, R., Renn, O., Slovic, P., Brown, H., Emel, J., Goble, R., Kasperson, J., and Ratick, S. (1988). The social amplification of risk: A conceptual framework. *Risk Analysis*, 8, 177-187.
- Katz, R., Parlange, M., and Naveau, P. (2002). Statistics of extremes in hydrology. *Advances in Water Resources*, 25, 1287-1304.
- Kramer, M., Terheiden, K., and Wieprecht, S. (2016). Safety criteria for the trafficability of inundated roads in urban floodings. *International Journal of Disaster Risk Reduction*, 17, 77-84.
- Koenig, J. (1980). Indicators of urban accessibility: Theory and application. *Transportation*, 9, 145-172.
- Kunkel, K., Andsager, K., and Easterling, D. (1999). Long-term trends in extreme precipitation events over the conterminous United States and Canada. *Journal of Climate*, 12, 2515-2527.
- Lu, Q., and Peng, Z. (2011). Vulnerability analysis of transportation network under scenarios of sea level rise. *Journal of the Transportation Research Board*, 2263, 174-181.
- Lu, Q., Peng, Z., and Zhang, J. (2015). Identification and prioritization of critical transportation infrastructure: case study of coastal flooding. *Journal of Transportation Engineering*, 141, 04014082.

- Maksimovic, C. (2009). Overland flow and pathway analysis for modelling of urban pluvial flooding. *Journal of Hydraulic Research*, 47, 512-523.
- Martínez-Gomariz, E., Gómez, M., Russo, B., and Djordjević, S. (2017). A new experiments-based methodology to define the stability threshold for any vehicle exposed to flooding. *Urban Water Journal*, 14, 930-939.
- Mattsson, L.G. (2007) Railway capacity and train delay relationships. In Murray A.T. & Grubestic T.H. (eds), *Critical Infrastructure* (pp.129-150). Berlin: Springer
- Mavoja, S., Witten, K., McCreanor, T., and O’Sullivan, D. (2012). GIS based destination accessibility via public transit and walking in Auckland, New Zealand. *Journal of Transport Geography*, 20, 15-22.
- McCarthy, S., Tunstall, S., Parker, D., Faulkner, H., and Howe, J. (2007). Risk communication in emergency response to a simulated extreme flood. *Environmental Hazards*, 7, 179-192.
- McLafferty, S. (2003). GIS and health care. *Annual Review of Public Health*, 24, 25-42.
- Miller, H. (1999). Measuring space-time accessibility benefits within transportation networks: basic theory and computational procedures. *Geographical Analysis*, 31, 187-212.
- Milrad, S., Gyakum, J., and Atallah, E. (2015). A meteorological analysis of the 2013 Alberta flood: Antecedent Large-Scale Flow Pattern and Synoptic–Dynamic Characteristics. *Monthly Weather Review*, 143, 2817-2841.
- Mitchell, L., and Romero, D. (2019). 'Unacceptable': Edmonton police takes responsibility for lengthy response to bloody assault. *CTV News Edmonton*. Available at: <https://edmonton.ctvnews.ca/unacceptable-edmonton-police-takes-responsibility-for-lengthy-response-to-bloody-assault-1.4534719> [Accessed August 7, 2019].

- Nicholson, A., and Dalziell, E. (2003). Risk evaluation and management: A road network reliability study, in Michael G. H. Bell, Yasunori Iida (ed.) *The Network Reliability of Transport*, pp.45-60.
- Niemeier (1997). A consumer welfare approach to measuring accessibility. *Transportation Research Part A: Policy and Practice*, 30, 84-85.
- Nirupama N. and Simonovic S. (2006) Increase of flood risk due to urbanisation: A Canadian example. *Natural Hazards* 40, 25-41.
- Novak, D., and Sullivan, J. (2014). A link-focused methodology for evaluating accessibility to emergency services. *Decision Support Systems*, 57, 309-319.
- Novotny, E. and Stefan, H. (2007.) Stream flow in Minnesota: indicator of climate change. *Journal of Hydrology*, 334, 319-333.
- O'Sullivan, D., Morrison, A., and Shearer, J. (2000). Using desktop GIS for the investigation of accessibility by public transport: an isochrones approach. *International Journal of Geographical Information Science*, 14, 85-104.
- Oh, K., and Jeong, S. (2007). Assessing the spatial distribution of urban parks using GIS. *Landscape and Urban Planning*, 82, 25-32.
- Open Calgary (2018a) 1:100 Flood Map (1% chance of occurring in any year). *Calgary*. Available at: <https://data.calgary.ca/Environment/1-100-Flood-Map-1-chance-of-occurring-in-any-year-/w8wn-kuii> [Accessed May 9, 2019].
- Open Calgary (2018b) Hydrology. *Calgary*. Available at: <https://data.calgary.ca/Environment/Hydrology/a2cn-dxht> [Accessed May 9, 2019].
- Open Calgary (2018c) Calgary Fire Stations. *Calgary*. Available at: <https://data.calgary.ca/dataset/Calgary-Fire-Stations/cqsb-2hhg> [Accessed May 9, 2019].

- Open Calgary (2018d) EMS Fire Stations. *Calgary*. Available at: <https://data.calgary.ca/Health-and-Safety/EMS-Stations/s6f4-ijrf> [Accessed May 9, 2019].
- Open Calgary (2018e) Calgary Police Service Office Locations. *Calgary*. Available at: <https://data.calgary.ca/Health-and-Safety/Calgary-Police-Service-Office-Locations/ap4r-bav3> [Accessed May 9, 2019].
- Páez, A., Scott, D., and Morency, C. (2012). Measuring accessibility: positive and normative implementations of various accessibility indicators. *Journal of Transport Geography*, 25, 141-153.
- Pederson, G., Gray, S., Ault, T., Marsh, W., Fagre, D., Bunn, A., Woodhouse, C. and Graumlich, L. (2011). Climatic controls on the snowmelt hydrology of the northern Rocky Mountains. *Journal of Climate*, 24, 1666-1687.
- Peterson, T., Zhang, X., Brunet-India, M., and Vázquez-Aguirre, J. (2008). Changes in North American extremes derived from daily weather data. *Journal of Geophysical Research*, 113.
- Pistrika, A., and Jonkman, S. (2009), Damage to residential buildings due to flooding of New Orleans after hurricane Katrina. *Natural Hazards*, 54, 413-434.
- Poesch, M., Chavarie, L., Chu, C., Pandit, S. and Tonn, W. (2016). Climate change impacts on freshwater fishes: A Canadian perspective. *Fisheries*, 41, 385-391.
- Pregolato, M., Ford, A., Wilkinson, S., and Dawson, R. (2017). The impact of flooding on road transport: A depth-disruption function. *Transportation Research Part D: Transport and Environment*, 55, 67-81.
- Public Safety Canada (2019a). Government of Canada funds flood mitigation project in Ontario. *Public Safety Canada*. Available at: <https://www.canada.ca/en/public-safety-canada/news/2019/05/government-of-canada-funds-flood-mitigation-project-in-ontario.html> [Accessed August 2, 2019].

Public Safety Canada (2019b). National Strategy for Critical Infrastructure. *Public Safety Canada*. Available at: <https://www.publicsafety.gc.ca/cnt/rsrscs/pblctns/srtg-crtcl-nfrstrctr/index-en.aspx> [Accessed July 29, 2019].

Public Safety Canada (2019c). Emergency Management. *Public Safety Canada*. Available at: <https://www.publicsafety.gc.ca/cnt/mrgnc-mngmnt/index-en.aspx> [Accessed May 17, 2019].

Rennó, C., Nobre, A., Cuartas, L., Soares, J., Hodnett, M., Tomasella, J., and Waterloo, M. (2008). HAND, a new terrain descriptor using SRTM-DEM: Mapping terra-firme rainforest environments in Amazonia. *Remote Sensing of Environment*, 112, 3469-3481.

Sarewitz, D., Pielke, R., and Keykhah, M. (2003). Vulnerability and risk: some thoughts from a political and policy perspective. *Risk Analysis*, 23, 805-810.

Schmitt, R. (1956). Estimating daytime populations. *Journal of the American Institute of Planners*, 22(2), 83-85.

Schnebele, E., Cervone, G., Kumar, S., and Waters, N. (2014). Real time estimation of the Calgary floods using limited remote sensing data. *Water*, 6, 381-398.

Sene, K. (2008). *Flood warning, forecasting and emergency response*, Berlin: Springer.

Shah, S., Mustaffa, Z., Martinez-Gomariz, E., Kim, D., and Yusof, K. (2019). Criterion of vehicle instability in floodwaters: past, present and future. *International Journal of River Basin Management*, 1-23.

Sharma, V., Al-Hussein, M., Safouhi, H., and Bouferguène, A. (2008). Municipal infrastructure asset levels of service assessment for investment decisions using analytic hierarchy process. *Journal of Infrastructure Systems*, 14, 193-200.

- Shiomi, Y., Seto, Y., and Uno, N. (2011). Model for location of medical facility and evaluation of vulnerability and accessibility of road network. *Transportation Research Record: Journal of the Transportation Research Board*, 2234, 41-48.
- Singh, P., Sinha, V., Vijhani, A., and Pahuja, N. (2018). Vulnerability assessment of urban road network from urban flood. *International Journal of Disaster Risk Reduction*, 28, 237-250.
- Smith, A., Bates, P., Wing, O., Sampson, C., Quinn, N., and Neal, J. (2019). New estimates of flood exposure in developing countries using high-resolution population data. *Nature Communications*, 10.
- Sohn, J. (2006). Evaluating the significance of highway network links under the flood damage: An accessibility approach. *Transportation Research Part A: Policy and Practice*, 40, 491-506.
- Stanfield, K. (2019). Why we're a far cry from the 2013 Flood. *CTV News Calgary*. Available at: <https://calgary.ctvnews.ca/why-we-re-a-far-cry-from-the-2013-flood-1.4476617> [Accessed September 3, 2019].
- Statistics Canada (2016). Census Profile, 2016 Census. *Statistics Canada*. Available at: <https://www12.statcan.gc.ca/censusrecensement/2016/dppd/prof/details/page.cfm?Lang=E&Geo1=CMACA&Code1=825&Geo2=PR&Code2=48&Data=Count&SearchText=calgary&SearchType=Begins&SearchPR=01&B1=All&TABID=1> [Accessed April 17, 2019].
- Suarez, P., Anderson, W., Mahal, V., and Lakshmanan, T. (2005). Impacts of flooding and climate change on urban transportation: A systemwide performance assessment of the Boston Metro Area. *Transportation Research Part D: Transport and Environment*, 10, 231-244.

- Sun, L., and Yin, Y. (2017). Discovering themes and trends in transportation research using topic modeling. *Transportation Research Part C: Emerging Technologies*, 77, 49-66.
- Sutherland, S. (2016). Three years later: What caused the 2013 Alberta floods?. *The Weather Network*. Available at: <https://www.theweathernetwork.com/news/articles/why-was-southern-alberta-so-vulnerable-to-flooding-in-2013/29800> [Accessed September 3, 2019].
- Taylor, M. A. P., and D'Este, G.M.D. (2003). Concepts of network vulnerability and applications to the identification of critical elements of transport infrastructure. *Paper presented at the 26th Australasian Transport Research Forum*, Wellington, New Zealand.
- Taylor, M. A. P. and D'Este, G.M.D. (2003) Network vulnerability: an approach to reliability analysis at the level of national strategic transport networks. In Bell M.G.H & Iida Y. (eds), *The Network Reliability of Transport* (pp.23-44). Kidlington: Elsevier Science
- Taylor, M., Sekhar S., and D'Este, G. (2006). Application of accessibility based methods for vulnerability analysis of strategic road networks. *Networks and Spatial Economics*, 6, 267-291.
- Taylor, M., and Susilawati (2012). Remoteness and accessibility in the vulnerability analysis of regional road networks. *Transportation Research Part A: Policy and Practice*, 46, 761-771.
- Thomas, M. (2013). How Large was the Flood in Calgary?. *Urban Workbench*. Available at: <https://urbanworkbench.com/how-large-was-the-flood-in-calgary/> [Accessed September 3, 2019].
- Transport Canada (2018) Road Transportation. *Government of Canada*. Available at: <https://www.tc.gc.ca/eng/policy/anre-menu-3021.htm> [Accessed July 13, 2019].

- United Nations (2018) 2018 Revision of World Urbanization Prospects. *United Nations Department of Economic and Social Affairs*. Available at: <https://www.un.org/development/desa/publications/2018-revision-of-world-urbanization-prospects.html> [Accessed July 10, 2019].
- Van Der Sande, C., De Jong, S., and De Roo, A. (2003). A segmentation and classification approach of IKONOS-2 imagery for land cover mapping to assist flood risk and flood damage assessment. *International Journal of Applied Earth Observation and Geoinformation*, 4, 217-229.
- Veiga, V., Hassan, Q., and He, J. (2014). Development of flow forecasting models in the Bow River at Calgary, Alberta, Canada. *Water*, 7, 99-115.
- Vincent, L., Zhang, X., Brown, R., Feng, Y., Mekis, E., Milewska, E., Wan, H. and Wang, X. (2015). Observed trends in Canada's climate and influence of low-frequency variability modes. *Journal of Climate*, 28, 4545-4560.
- Viswanath, K., and Peeta, S. (2003). Multicommodity maximal covering network design problem for planning critical routes for earthquake response. *Transportation Research Record: Journal of the Transportation Research Board*, 1857, 1-10.
- Westra, S., Fowler, H., Evans, J., Alexander, L., Berg, P., Johnson, F., Kendon, E., Lenderink, G., and Roberts, N. (2014). Future changes to the intensity and frequency of short-duration extreme rainfall. *Reviews of Geophysics*, 52, 522-555.
- Yang, D., Goerge, R., and Mullner, R. (2006). Comparing GIS-based methods of measuring spatial accessibility to health services. *Journal of Medical Systems*, 30(1), 23-32.
- Yin, J., Yu, D., Yin, Z., Liu, M., and He, Q. (2016). Evaluating the impact and risk of pluvial flash flood on intra-urban road network: A case study in the city center of Shanghai, China. *Journal of Hydrology*, 537, 138-145.

- Yourex, H. (2018). AHS sets new 12 minute ambulance response time targets. *Global News*. Available at: <https://globalnews.ca/news/2407857/ahs-sets-new-12-minute-ambulance-response-time-targets/> [Accessed May 17, 2019].
- Youssef, A., Pradhan, B., and Hassan, A. (2010). Flash flood risk estimation along the St. Katherine road, southern Sinai, Egypt using GIS based morphometry and satellite imagery. *Environmental Earth Sciences*, 62, 611-623.
- Yücel, E., Salman, F., and Arsik, I. (2018). Improving post-disaster road network accessibility by strengthening links against failures. *European Journal of Operational Research*, 269, 406-422.
- Zhu, X., and Liu, S. (2004). Analysis of the impact of the MRT system on accessibility in Singapore using an integrated GIS tool. *Journal of Transport Geography*, 12, 89-101.
- Whitfield, P. and Pomeroy, J. (2016). Changes to flood peaks of a mountain river: implications for analysis of the 2013 flood in the Upper Bow River, Canada. *Hydrological Processes*, 30, 4657-4673.

Appendix

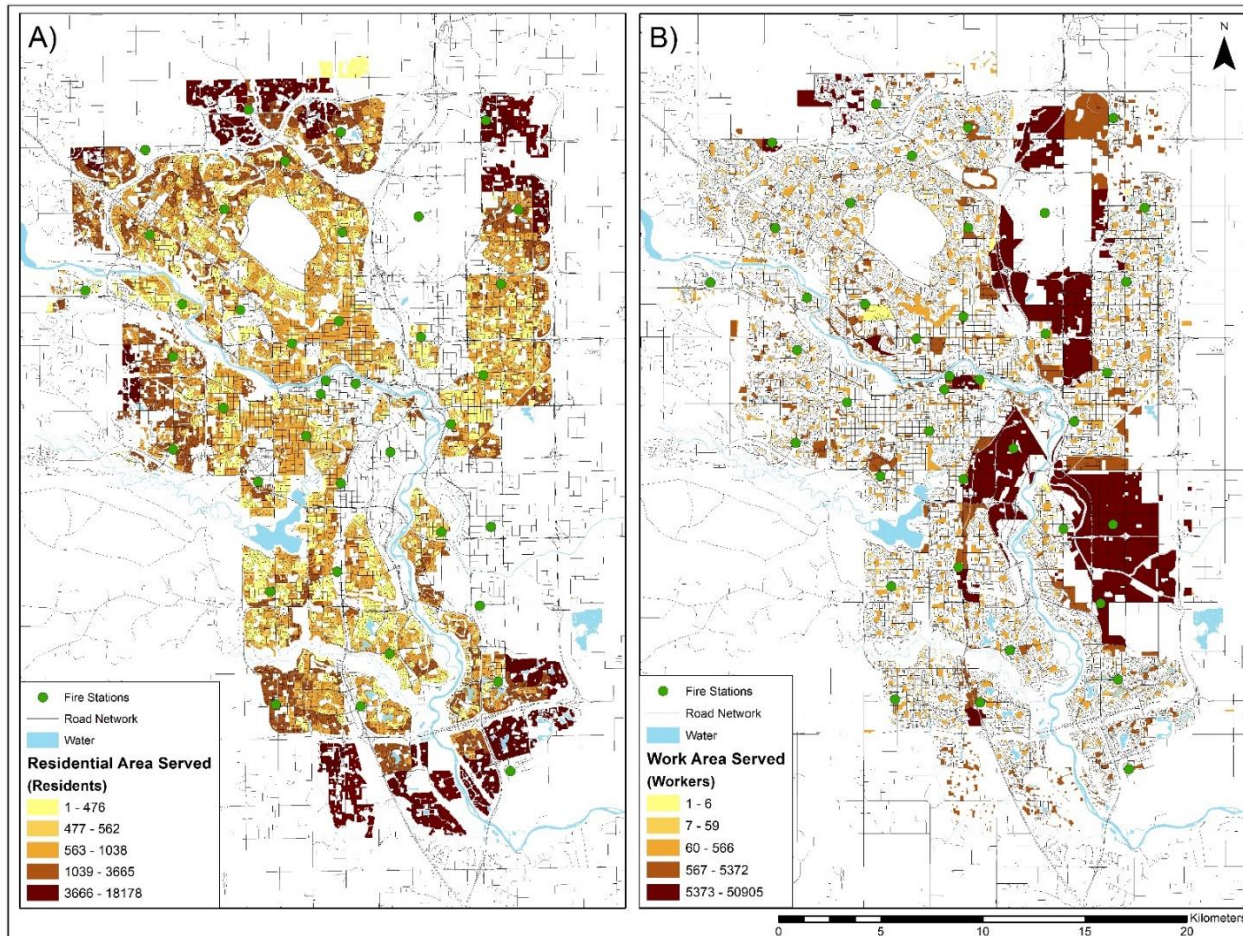


Figure 12. Base case representing (A) residents and (B) workers served by fire within the 12-minute threshold.

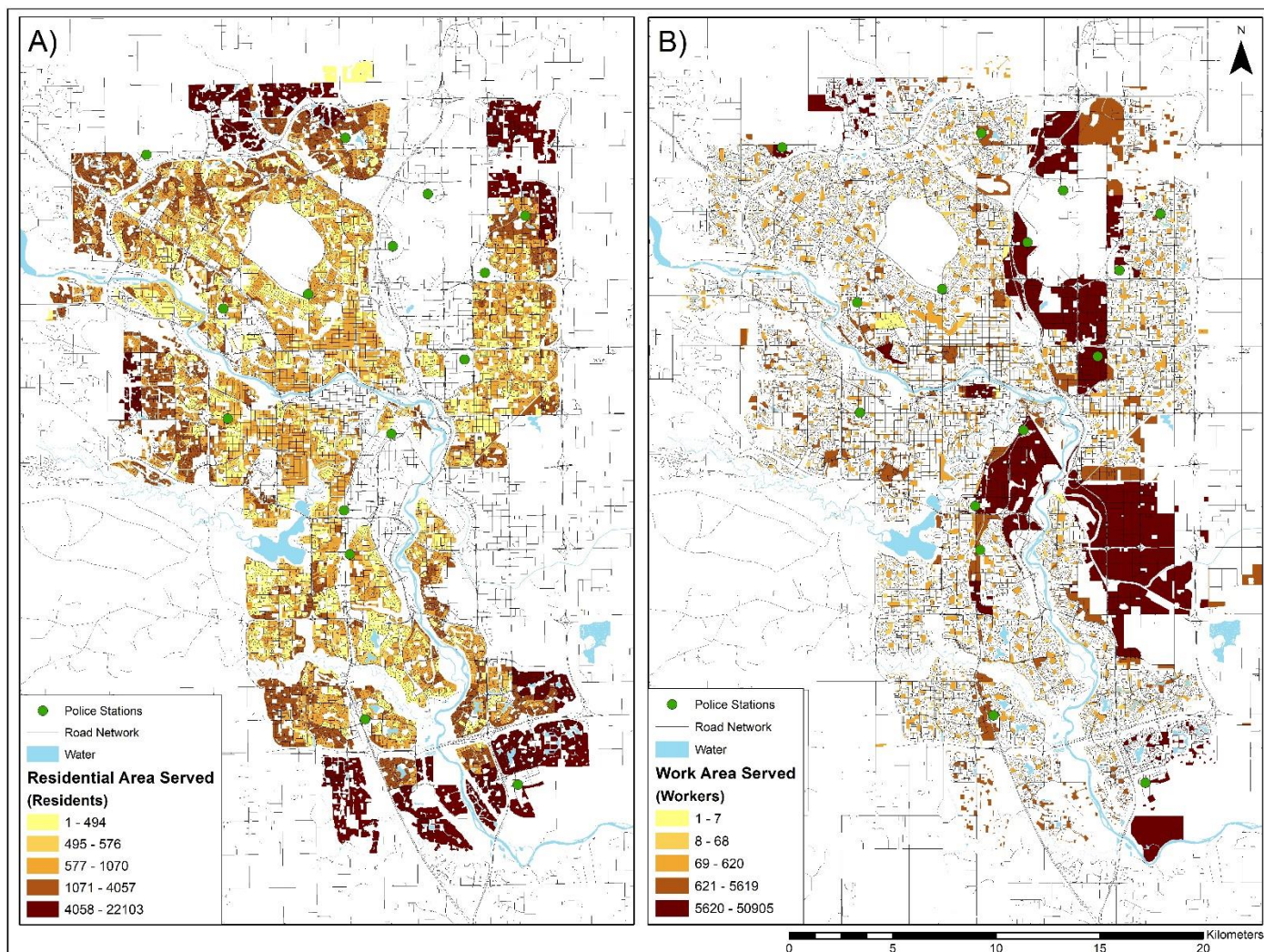


Figure 13. Base case representing (A) residents and (B) workers served by police within the 120-minute threshold.